MICROBIOTA AND TELOMERE SHORTENING IN GUT-LUNG AXIS OF HUMAN IMMUNODEFICIENCY VIRUS INFECTED DONORS

by

SHUN-WEI JULIA YANG

B.M.L.Sc., The University of British Columbia, 2016

A THESIS SUBMITTED IN PARTIAL FULFILLMENT OF

THE REQUIREMENTS FOR THE DEGREE OF

MASTER OF SCIENCE

in

THE FACULTY OF GRADUATE AND POSTDOCTORAL STUDIES

(Experimental Medicine)

THE UNIVERSITY OF BRITISH COLUMBIA

(Vancouver)

October 2018

Committee Page

The following individuals certify that they have read, and recommend to the Faculty of Graduate and Postdoctoral Studies for acceptance, a thesis/dissertation entitled:

Microbiota and telomere shortening in gut-lung axis of human immunodeficiency virus infected donors

submitted by Shun-Wei Julia Yang in partial fulfillment of the requirements for

the degree of Master of Science

in Experimental Medicine

Examining Committee:

Dr. Don D. Sin
Supervisor

Dr. Paul Man
Supervisory Committee Member

Dr. Janice Leung
Supervisory Committee Member

Dr. Pascal Bernatchez
External Examiner

Abstract

Previous studies have demonstrated the existence of a gut-lung axis and its proposed role in altering immune response and respiratory disease pathogenesis. The lung and gut microbiomes have been individually studied in the context of Human Immunodeficiency Virus (HIV) infection; however the gut-lung axis in HIV remains relatively unexplored and requires further investigation. This study examined the microbiomes of the gut-lung axis and telomere attrition in HIV subjects using paired human lung and small intestine tissue.

Paired lung and small intestine tissue autopsy specimens were obtained from ART-treated HIV-positive and HIV-negative donors through the National NeuroAIDS Tissue Consortium. Frozen samples were sectioned on dry ice and weighed for DNA extraction using the QIAGEN DNeasy® Blood and Tissue kit. Droplet digital PCR was used to measure bacterial load and quantitative PCR was performed to determine absolute telomere length (aTL). The 16S rRNA V4 region was sequenced using the MiSeq sequencing platform. Extraction negatives were run through the entire workflow alongside samples for quality control. Raw sequence reads were processed using QIIME2 (Quantitative Insights Into Microbial Ecology 2, v2018.2) followed by statistical analysis using R studio. Several t-tests, linear regression, PERMANOVA and ANCOVA were used for statistical analysis.

Microbial composition was not found to differ significantly between ART-treated HIV-positive and HIV-negative donors in both lung and small intestine. However, bacterial load and abundance of individual amplicon sequence variants (ASVs) were found to be correlated in the lung and small intestine. Bacteroides was decreased in ART-treated HIV-positive donors and

identified as one of the bacteria most likely to help explain differences between HIV-negative and ART-treated HIV-positive microbiomes. Telomere length was demonstrated to be shortened in lungs of ART-treated HIV-positive donors in comparison to HIV-negative but no differences were found between the two groups in the small intestine.

ART-treated HIV donors present microbiomes similar to HIV-negative donors, suggesting that ART can provide the microenvironment necessary to maintain a “healthy” microbiome. Furthermore, microbiomes of the gut-lung axis have demonstrated a correlation in bacterial load and abundance of individuals ASVs, suggesting a strong relationship between the two sites in both ART-treated HIV donors and HIV-negative donors.

Lay Summary

Previous studies have demonstrated the existence of a gut-lung axis and its proposed role in altering the immune response and respiratory disease pathogenesis. While the lung and gut bacterial communities, known as microbiomes, in HIV infection have been studied individually, the gut-lung axis in HIV is relatively unknown and still remains to be explored. My project examines the microbiomes of the gut-lung axis in HIV subjects using paired human lung and small intestine tissue. Specifically, the effect of HIV infection on the microbial composition of lung and small intestine while accounting for characteristics such as CD4 count, viral load and telomere length will be investigated.

Preface

This research was approved by the UBC-Providence Health Care Research Ethics Board (certificate number H15-02807).

Identification and design of the research program was done by Dr. Don Sin, Dr. Paul Man, Dr. Janice Leung and I. All droplet digital PCR and quantitative PCR experiments and data analysis were conducted by myself. Library preparation was completed by technician David Ngan and I. Sequencing by MiSeq was performed at the UBC Sequencing and Bioinformatics Consortium by Dr. Sunita Sunha on a fee-per-library service.

Table of Contents

List of Tables

List of Figures

List of Abbreviations

16S: 16 Svedberg Units

AIDS: acquired immunodeficiency syndrome

ANCOVA: analysis of covariance

ANOVA: analysis of variance

AP-1: activator protein 1

ART: antiretroviral therapy

ASV: amplicon sequence variant

aTL: absolute telomere length

AZT: zidovudine

BAL: bronchoalveolar lavage

CCR5: C-C chemokine receptor type 5

Cq: quantitation cycle

COPD: chronic obstructive pulmonary disease

CXCR4: chemokine receptor type 4

ddPCR: droplet digital polymerase chain reaction

DNA: deoxyribonucleic acid

dsDNA: double-stranded deoxyribonucleic acid

EDTA: Ethylenediaminetetraacetic acid

F: Forward

GOLD: Global Initiative for COPD

HAART: highly active antiretroviral therapy

HAND: human immunodeficiency virus-associated neurocognitive disorders

hBD-2: human beta defensin-2

HID: human infectious dose

HIV: human immunodeficiency virus

HIV -: HIV-negative

HIV +: HIV-positive

IBD: inflammatory bowel disease

IBS: irritable bowel syndrome

LEfSe: Linear discriminant analysis effect size

LHMP: Lung HIV Microbiome Project

LPS: lipopolysaccharide

NF-κB: nuclear factor- κB

NMDS: non-metric multidimensional scaling

OD: optical density

OUT: operational taxonomic unit

PCoA: principal coordinate analysis

PCR: polymerase chain reaction

PERMANOVA: permutational multivariate analysis of variance

PLWH: persons living with human immunodeficiency virus

qPCR: quantitative polymerase chain reaction

R: reverse

RNA: ribonucleic acid

rRNA: ribosomal ribonucleic acid

SCFA: short chain fatty acid

Tris-Cl: tris(hydroxymethyl)aminomethane hydrochloride

WHO: World Health Organization

Acknowledgements

First, I would like to thank my supervisor, Dr. Don Sin, for all his support and guidance during my time as an undergraduate and graduate student. I have learnt so much during my time here and have been inspired by his conscientiousness and dedication to his craft.

Second, I would like to thank Dr. Paul Man and Dr. Janice Leung for all their patient guidance and encouragement. Their advice and support have been invaluable to the completion of this project. I am grateful to Dr. Pascal Bernatchez for his insights and suggestions, helping me to view this project in a different sense, away from the wet and dry labs.

Third, I would like to thank both current and former members of the Sin lab for all their help and support. Special thanks to Dr. Marc Sze for inspiring me with his enthusiasm and dedication to his research and taking the time and painstaking effort to train me during my initial summers. I am grateful to Dr. Fernando Studart for all his help in navigating the confusing world of bioinformatics. Of course, thank you to our wonderful technicians Sheena Tam and David Ngan for all they have done for the lab and always being ready to offer their time and expertise. Thank you to David Jaw and Anthony Tam for all their wise advice on matters both in and outside the lab. I would also like to thank my fellow students Nancy Yang, Minhee Jin and Kimia Shahangian for making my time in the lab joyful.

Lastly, I would like to thank my family for their never ending love and support. I am grateful to have the great fortune of being their daughter and little sister.

This work was supported by a CIHR grant held by Dr. Paul Man.

This thesis was made possible from NIH funding through the NIMH and NINDS Institutes by the following grants:

Texas NeuroAIDS Research Center: U24MH100930
California NeuroAIDS Tissue Network: U24MH100928
National Neurological AIDS Bank: U24MH100929
Manhattan HIV Brain Bank: U24MH100931
Data Coordinating Center: U24MH100925

Its contents are solely the responsibility of the authors and do not necessarily represent the official view of the NNTC or NIH

To my dearest family

Chapter 1: Background

1.1 Human Immunodeficiency Virus

1.1.1 Epidemiology and History

According to the UNAIDS 2017 global HIV statistics, an estimated 36.9 million people worldwide are living with HIV[1]. Since the start of the HIV pandemic in the early 1980's, 77.3 million people have been infected with HIV and 35.4 million people have died from AIDS-related illnesses[1]. In 2017, 1.8 million people were newly infected, 940,000 died from AIDS-related illnesses and 21.7 million people were accessing antiretroviral therapy[1]. The World Health Organization (WHO) African region has the highest HIV population with 4.1% adults living with HIV, accounting for almost two-thirds of all people living with HIV worldwide[2]. In Canada, 84,409 cases of HIV have been reported since 1985 with variations in provincial and territorial HIV diagnosis rates[3].

The HIV pandemic originated from zoonotic infections of simian immunodeficiency viruses from African primates with HIV-1 being transmitted by Central African chimpanzees and HIV-2 by West African sooty mangabeys[4]. The spread of HIV-1 main (M) subtypes have led to a global pandemic while HIV-2 has been relatively restricted to West Africa and with low prevalence, to Europe, South America and Asia[5]. In Canada, the most common subtype is HIV-1 subtype B, making up 79.6% of the 1,811 specimens genotyped in the Canadian HIV Strain and Drug Resistance Surveillance Program (SDR Program) initiated by the Public Health Agency of Canada (PHAC)[6].

HIV was first officially reported in 1981 when cases of Pneumocystis carinii pneumonia, a rare lung infection, were described in five previously healthy, young, gay males by the U.S.

Centers for Disease Control and Prevention (CDC)[7]. The disease was named Acquired Immune Deficiency Syndrome (AIDS) in 1982 and the first case in Canada was reported in March of that year[8]. Reports of HIV were first described in homosexual men then intravenous drug users, blood transfusion recipients and heterosexual individuals[7]. HIV was first isolated by Dr. Françoise Barré-Sinoussi and Dr. Luc A. Montagnier at the Pasteur Institute (Paris, France) in 1983 and then implicated to be the cause of AIDS by Dr. Robert Gallo and colleagues at the National Cancer Institute (Maryland, US) in 1984[7]. The US Food and Drug Administration (FDA) approved the first antiretroviral drug, zidovudine (AZT) in 1987, leading the way to the introduction of antiretroviral therapy (ART) in 1995[7].

ART has become the standard treatment for HIV infection since 1996, achieving this through the use of different combinations of drugs[9,10]. Standard ART consists of at least three medications (known as highly active antiretroviral therapy or HAART)[9,10]. Potential medications include reverse transcriptase inhibitors, fusion inhibitors, protease inhibitors, chemokine receptor 5 antagonists and integrase strand transfer inhibitors[9]. Effective ART controls HIV multiplication in infected patients, and increases or maintains CD4 count, allowing a prolonged asymptomatic phase and decelerating disease progression[11]. Furthermore, ART reduces the risk of transmission when viral load is kept at undetectable levels[11]. In Canada, a 20-year-old HIV patient on ART can be expected to live into their early 70s, approaching the life expectancy of the general population[12]. However, differences to life expectancy vary based on race, sex, HIV transmission risk group and CD4 count[12]. Based on results from the Strategic Timing of Antiretroviral Therapy (START) trial, the WHO has recommended for all people living with HIV to initiate ART as soon after diagnosis as possible[13]. The START trial presented conclusive evidence that

initiation of ART soon after HIV diagnosis reduces risk of serious illnesses such as Kaposi's sarcoma and tuberculosis[14].

1.1.2 Overview of HIV

HIV is an enveloped ribonucleic acid (RNA) virus classified as part of the Lentivirus genus in the Retroviridae family and Orthoretrovirinae subfamily. The virus consists of two identical single-stranded RNA molecules enclosed within a conical capsid assembled from inner capsid protein p24, followed by a symmetrical outer capsid membrane formed by matrix protein, then viral lipid bilayer envelope and outer lipid membrane envelope[4]. HIV is present in blood, semen, vaginal secretions and breast milk and can enter the body via eczematous or damaged skin or mucosa, mucous membranes, transplanted organs and parenteral inoculation[15]. High risk populations in Canada include men who have sex with men (MSM), injection drug users, people from countries where HIV is endemic and indigenous people[6].

HIV targets activated CD4 T lymphocytes and enters the cells through interactions with CD4 and chemokine co-receptors C-C chemokine receptor type 5 (CCR5) or C-X-C chemokine receptor type 4 (CXCR4)[9,10,16]. One human infection dose (HID) is approximately 500 to 1,000 HIV particles with a higher amount required for infection through mucous membranes in comparison to infection via bloodstream[4]. Confirmatory tests in Canada target anti-HIV antibodies, HIV p24 antigen or HIV RNA while CD4 count (cells per mm^3) and viral load (copies of virus per mL) help monitor disease progression[3].

Clinical progression of HIV occurs in three stages: acute HIV infection, clinical latency and AIDS. After primary infection, people develop acute HIV syndrome in which the virus is

widely disseminated and seeded into lymphoid organs. During this period, flu-like symptoms may occur and high viral loads are found in the blood, making people at this stage very contagious. This is followed by clinical latency in which HIV is inactive or dormant. Patients on ART may experience this stage for decades but patients not on therapy may progress to AIDS in 2 to 25 years or longer. Towards the end of this stage, viral load increases and CD4 cell count decreases. In the final stage, people develop AIDS and display a weakened immune response, opportunistic infections and malignant neoplasms. Opportunistic infections include pneumocystis pneumonia (PCP), toxoplasmosis, cytomegalovirus retinitis and mycobacterium tuberculosis. Common neoplasms observed in HIV infections are human herpes virus type 8 (HHV-8) associated Kaposi's sarcoma, non-Hodgkin's lymphomas and human papillomavirus (HPV) induced cervical carcinoma[4,10,16,17].

1.2 Microbiome

1.2.1 Introduction

The human body contains an approximated 38 trillion bacterial cells compared to the 30 trillion human cells estimated based on a 70 kg "reference man"[18]. These bacteria are found throughout the human body in variable quantities, inhabiting areas such as the gastrointestinal tract, skin, lungs and oral cavity[19]. Microbiota is the term used for a community of microorganisms including bacteria, viruses, archaea and fungi that inhabit a specific location at a specific point in time while the microbiome refers to the genetic material of the microbiota. Both terms have been frequently used in studies to encompass only the bacterial components and are often used interchangeably[19]. With the abundance of bacteria and corresponding microbiota in

the human body, it is important to understand the roles of these communities in health and disease processes and interactions within and between communities.

Studies on the microbiome have rapidly increased since 2009 due to the emergence and significantly reduced costs of culture-independent, high-throughput methods such as next-generation sequencing along with the development of molecular phylogenetic approaches to organize taxonomic diversity. With the discovery of 16S ribosomal RNA, researchers are able to classify sequences in the form of amplicon sequence variants (ASVs) or operational taxonomic units (OTUs) using 16S databases such as SILVA, Greengenes and RDP for taxonomic identification[20–23].

The interaction between environmental microbiota and various human body sites is highly dynamic, leading to changes in human microbiome due to different birthing methods (vaginal delivery versus caesarean section), dietary changes and disease onset and progression[19,24,25]. One study demonstrated that infants delivered vaginally had microbiomes resembling their mother's vaginal microbiomes while microbiomes of caesarean section infants consisted on bacteria found on the skin surface[24]. Another study showed that it was possible to link a computer mouse to the person's hand that had used it with up to 95% accuracy after comparing to a database of other hands[26].

Previous studies have shown that microbiota are important in metabolism, immunological processes and disease outcome and mechanism. Germ-free mice inoculated with gut microbiota from wild-type mice demonstrated increased energy extraction from diet, leading to increased energy deposition into adipocytes without increases in food intake. E. coli Nissle and lactobacilli

were shown to induced antimicrobial peptide human beta defensin-2 (hBD-2) expression by gut epithelial cells through proinflammatory pathways including nuclear factor- κB (NF-κB) and activator protein 1 (AP-1). Through hBD-2, E. coli Nissle and lactobacilli strengthen the intestinal barrier by counteracting bacterial adherence and invasion. Many studies have presented an inverse relationship between rates of childhood asthma and exposure to microbially rich environments during infancy such as growing up on a farm with livestock[27–29], living with two or more dogs[30] and drinking non-pasteurized milk[31].

The Human Microbiome Project was launched in 2008 by the U.S. National Institutes of Health to better understand the impact of microbiomes on human health and disease. The first phase (2008 to 2012) focused on charactering human microbiome and involved 300 healthy individuals, 18 body sites, 5 body regions, resulting in 11,000 primary specimens for sequencing[32–34]. The focus of the second phase (2014 to 2017), the Integrative Human Microbiome Project, was to develop resources to characterize the microbiome and distinguish its role in health and disease[35]. Since 2009, publications on the microbiome have rapidly increased to over 8,700 papers published in 2017.

1.2.2 Gut Microbiome

The gut microbiome is one of the earliest and most extensively studied microbiomes in both health and disease due to the abundance of microorganisms in faecal matter which is commonly used in these studies and easily attainable. In the first year of life, microbiome diversity increases until around 2.5 years in which the composition, diversity and functional capabilities resemble that of the adult microbiome[36,37]. It is not clear whether the gut microbiome shifts later on in life as one study demonstrated an increased abundance of Bacteroidetes in

subjects over 65 years old while another study showed that the microbiome was relatively comparable in subjects over 70 years old to the younger cohort[38,39]. However, studies have shown that in the elderly, the gut microbiome displays a decreased capacity for metabolic processes like short chain fatty acid (SCFA) production and amylolysis and increased proteolytic activity[40]. The most common phyla in the gut microbiome are Proteobacteria, Firmicutes, Actinobacteria and Bacteroidetes[36,41,42].

Many factors are responsible for shaping the gut microbiota including diet, environmental factors, host immune system and physiological properties[25,36]. Diet is one of the major determinants of gut microbiome composition. Large alterations in the gut microbiome were observed between people on animal-based versus plant-based diets. Animal-based diets had decreased levels of Firmicutes, responsible for metabolising dietary plant polysaccharides and increased abundance of bile-tolerant bacteria such as Bacteroides and Alistipes[43]. Environmental factors that may affect the composition of the gut microbiome include surgery, geographical location, urban versus rural accommodations and depression[36,44–46]. Antibiotic usage can cause both short and long-term disruptions to the gut microbiome with studies demonstrating decreased richness and diversity[47]. The host immune system prevents opportunistic infections of host tissue by stratifying and compartmentalizing bacteria[48,49]. Secretory IgA helps limit exposure of epithelial cells to bacteria by co-localising with gut bacteria in the mucus layer[50]. Paneth cells in the epithelial layer of the small intestine produce antimicrobials such as lipopolysaccharide-binding protein, lysozomes and cathelicidins[51]. Physiological properties such as chemical, nutritional and immunological gradients influence microbial density and composition[52]. For example, bacterial growth is limited in the small intestine to facultative anaerobes with rapid

growth due to its high acidity, short transit time and presence of oxygen and antimicrobials, while the colon consists mainly of anaerobes that have the ability to break down complex carbohydrates that are not digested in the small intestine[52].

In health, the gut microbiota provides nutrients, maintains barrier integrity, protects against pathogens, influences metabolic homeostasis and regulates host immune response[53]. Nutrients provided by the gut microbiota include vitamin B12 produced by lactic acid bacteria, vitamin K, biotin, riboflavin and folate which is produced by Bifidobacteria and involved in DNA synthesis and repair[54–57]. Bacteria implicated in maintaining barrier integrity include Lactobacillus plantarum, Akkermansia muciniphila as well as Lactobacilli rhamnosus which promotes cell renewal and wound healing[58–60]. The healthy gut microbiota protects against colonisation by pathogenic bacteria by competing for attachment sites and nutrient sources and producing antimicrobial substances[61]. Bacteria in the colon break down complex carbohydrates using carbohydrate-active enzymes to generate short chain fatty acids (SCFA) which are involved in chemotaxis, apoptosis, proliferation and help regulate gene expression and the immune response[62]. Furthermore, the gut microbiome has been shown to be important in the development of the immune system. Germ-free mice demonstrated an absence of CD4+ T cell population expansion that could be reversed by treatment with polysaccharide A from Bacteroides fragilis[63]. Perturbations in the gut microbiota have been linked to a wide range of conditions including inflammatory bowel disease, irritable bowel syndrome, Clostridium difficile infection and obesity[61].

1.2.2.1 Gut Microbiome in HIV Infection

Based on current literature, the gut microbiome differs in HIV-negative, HIV-positive and ART-treated individuals although it is unclear the extent to which HIV infection alters the gut microbiome[64–68]. Various studies have characterized different patterns of composition for each study group. Confounding factors mentioned above such as diet and environmental factors as well as ART, antibiotic use and sexual practices may help explain the differing patterns of gut microbiome composition observed in separate studies. Additionally, level of bacterial classification examined and varying methods of samples collection including stool, tissue biopsy, rectal sponge and stool swabs may also influence the composition of the gut microbiome identified.

Enriched genus Prevotella and decreased Bacteroides in HIV-positive subjects in comparison to HIV-negative subjects have been demonstrated in several studies using both stool and mucosal biopsy samples[69–72]. Conversely, in a study from Uganda where transmission is predominately heterosexual, Prevotella was not found to be elevated in stool samples of HIV-infected subjects. However, HIV-negative subjects at baseline had a Prevotella-predominant stool microbiome, potentially due to differences in diet, which may have made it difficult to detect small increases in Prevotella[73]. In a Swedish cohort, Nowak et al did not observe an overabundance of Prevotella at baseline although abundance of Prevotella decreased after ART initiation[74]. Noguera-Julian et al demonstrated that the increased Prevotella and decreased Bacteroides enterotype was associated with MSM sub-group irrespective of HIV infection[75]. Increased abundance of Proteobacteria has been observed in HIV-positive subjects in several studies using mucosal samples[70,76]. Current literature is inconclusive on whether HIV infection

reduces microbial diversity as several studies have demonstrated a decrease in diversity while others have not.

With ART, the gut microbiome shifts towards a composition more similar to HIV-negative controls in comparison to untreated HIV-positive subjects. It has been suggested that unmanaged viral replication drives mucosal inflammation leading to changes in microbial composition which may be potentially reversed with ART and the subsequent recovery of the mucosal immune system[77].

1.2.3 Lung Microbiome

With the development of culture-independent techniques for microbial identification, the lungs which have previously been considered as sterile in health are now recognized to host diverse and dynamic communities of bacteria. The composition of the lung microbiome is dependent on immigration, elimination and regional growth conditions[78]. Microbial immigration occurs with microaspiration, direct mucosal dispersion and inhalation of bacteria. Microbial elimination is mediated by cough, mucociliary clearance and innate and adaptive host responses. Regional growth conditions include multiple factors such as pH, temperature, nutrients, competition from local microbes and interaction with host epithelial cells. In health, immigration and elimination are the two main driving forces behind lung microbiota but in disease states such as chronic inflammatory lung diseases and especially during exacerbations, the influence of regional growth conditions increases[78].

Within the lung, the composition and abundance of bacterial populations vary based on the anatomical location such as nasal, tracheal, bronchial or alveolar. In the nasal cavity, the

major bacterial phyla are Firmicutes, Proteobacteria, Bacteroidetes and Actinobacteria while typical bacterial genera include Moraxella, Streptococcus and Staphylococcus[79]. The most common phyla of the respiratory tract are Bacteriodes, Firmicutes, Proteobacteria and the most prevalent genera include Fusobacteria, Prevotella, Streptococcus, Pseudomonas and Veillonella[78]. In a study by Erb-Downward et al, bronchoalveolar lavage (BAL) samples and four to eight distinct tissue samples from each lobe were analyzed and demonstrated regional differences in the lung bacterial microbiome within an individual subject[80]. Previous studies have shown that bacterial communities in the lung are small in number but diverse[80–83].

The microbiome varies in composition between healthy people but also between healthy people and patients with chronic inflammatory lung diseases such as chronic obstructive pulmonary disease (COPD), asthma and cystic fibrosis[80,84–87]. Studies comparing the lung microbiome in states of health and disease have suggested shifts of microbial composition in the diseased lung. In asthma, the microbial composition in BAL samples shifts away from Bacteroidetes towards Proteobacteria[88]. In comparing COPD lung tissue samples with control, Sze et al found an increase in the Firmicutes phylum due to an increase in the Lactobacillus genus in patients with very severe COPD (Global Initiative for COPD [GOLD] 4)[86].

However, it is still unclear whether chronic diseases are drivers of microbiota imbalance or if microbiota composition contributes to disease pathology. Understanding the relationship between the lung microbiome and the host in health and disease may provide the knowledge required to develop therapeutic targets or supplements to help restore important microbial species and improve lung health.

1.2.3.1 Lung Microbiome in HIV Infection

The NIH Lung HIV Microbiome Project (LHMP, 2009 to 2015) encompassed 6 clinical sites and was created to characterize the lung and respiratory tract microbiomes in order to better understand the changes and effects of the microbiome in health and disease.

Studies under the LHMP have shown the lung microbiome to be similar between HIV-uninfected patients and HIV-infected patients with relatively preserved CD4 cell counts[89–92]. However, BAL from untreated patients with advanced HIV infection demonstrated a decrease in alpha diversity (richness and diversity) and greater beta diversity in comparison to BAL from HIV-uninfected patients. These differences were mitigated with the use of HAART but were still present up to 3 years after initiation of therapy[89]. In a study by Twigg III et al, an increased abundance of Streptococcus was found in the HIV population while Flavobacterium was increased in the control population[89]. When comparing the lung microbiome of BAL from patients with advanced HIV infection and without HIV infection at baseline and after 1 year of HAART, advanced HIV patients demonstrated an increased relative abundance of Prevotella and Veillonella which are associated with lung inflammation[89]. In particular, the genus Prevotella was associated with Th17 inflammation, development of COPD and pneumonia treatment and outcomes[93]. Tropheryma whipplei was found to be more frequent in the BAL of HIV-positive patients and ART lead to a reduction in relative abundance of T. whipplei in the lung which was hypothesized to originate from the gut[92].

The incidence of bacterial pneumonia is 5% to 30% in HIV infected patients in comparison to less than 1% in immunocompetent individuals[94–97]. Iwai et al demonstrated that bacterial pneumonia in HIV infected patients were enriched with phylogenetically diverse

bacteria including Firmicutes and Prevotellaceae while HIV-uninfected pneumonia was primarily enriched with Proteobacteria[98]. Alterations in the lung microbiome during HIV infection may contribute to lung complications and chronic inflammation.

1.2.4 Gut-Lung Axis

Patients with chronic lung diseases such as COPD and asthma have increased prevalence of gastrointestinal diseases including inflammatory bowel disease (IBD) and irritable bowel syndrome (IBS)[99,100]. The recently proposed gut-lung axis may help in understanding this phenomenon. Previous studies have shown that disturbance of gut microbiota by infection or antibiotics can change inflammatory signals normally released by the microbiota, contributing to an altered immune response. Exposure to structural ligands such as lipopolysaccharide (LPS) and secreted metabolites from the healthy gut microbiota maintains a homeostatic immune response that is altered when pathogenic bacteria and metabolites stimulate circulating lymphocytes, leading to changes in systemic immune responses[101]. Disturbances to gut microbiota during the development of the immune system in the early years can substantially alter the immune response and may potentially lead to chronic inflammatory disorders of the gut and lung later on in life[101]. Studies using germ-free mice have demonstrated underdeveloped immune systems and mucosal alterations that can be restored through gut microbiota colonization[102,103].

Proposed mechanisms of bacterial translocation between the gut and lung include ingested bacteria entering the lungs from the gastrointestinal tract through aspiration and direct transfer of bacteria from gut to lungs as observed when intestinal barrier integrity is compromised during sepsis and acute respiratory distress syndrome[104]. Entry of bacterial components and metabolites into the circulatory system can cause systemic inflammation[101].

The gut-lung axis has been proposed to play a role in respiratory diseases. Risk of asthma development was shown to be elevated when the gut microbiota contained increased abundance of Bacteroides fragilis and total anaerobes in the early years of life[104]. Mice with absent or depleted gut microbiota presented an impaired immune response and worsened outcomes after bacterial or viral respiratory infection[104]. Gut-specific Helicobacter pylori has been linked to decreased incidence of asthma and allergy but positively associated with COPD, suggesting that H. pylori and its subsequent systemic immune response may play different roles in different lung diseases[105–108].

Trompette et al demonstrated that short chain fatty acids (SCFA) originating from gut microbiota can affect the immune response in the lung through reducing dendritic cell promotion of Th2 proliferation by T cells[109]. Oral administration of SCFA has also been shown to have anti-inflammatory effects that reduced pulmonary pathology post bacterial and viral infection in mice[109]. Administration of segmented filamentous bacteria (SFB) in the gut has been shown to stimulate T helper 17 response and improve resistance to Staphylococcus aureus pneumonia[110–112]. In a study by Sze et al, instillation of LPS intratracheally in the lungs led to acute changes in the gut microbiome composition demonstrating that perturbations in the lung could also lead to changes in the gut microbiome[113].

Further research on causal links in the gut-lung axis may lead to the development of prophylactic or interventional strategies to modify the microbiota or immune response to improve patient quality of life. While there have been no studies on the gut-lung axis in HIV infection thus far, research on the effects of gut microbiota on the systemic immune response

may help in understanding its potential in mitigating chronic pulmonary diseases of which are more common in HIV patients.

1.3 HIV and Aging

1.3.1 Age-Related Diseases in HIV

With the introduction of ART, HIV patients are living longer and HIV prevalence is increasing worldwide despite a decrease in new infections. Average age for patients living with HIV (PLWH) continues to increase with more than 10% of this population over 50 years of age[113]. The emergence of an older HIV population at risk of chronic diseases makes it necessary to study the impact of HIV infection on aging and development of chronic diseases.

Even with controlled viral titres and preserved CD4 count, inflammation is elevated in HIV-positive patients and is associated with increased rates of renal, cardiovascular, neurocognitive, oncological and osteoporotic diseases[114–117]. Mechanisms through which inflammation is increased in HIV-positive patients includes low level viral replication in tissue, chronic reactivation of herpes viruses, microbial translocation and immune dysregulation due to depletion of CD4 T cells and increased senescent CD8 T cells[76,118–120].

Whether or not accelerated aging occurs in HIV patients is still a topic of debate. HIV-positive patients experience persistently elevated inflammatory markers, senescent immune changes and increased rates of chronic co-morbidities, geriatric syndromes and frailty[121]. However, in some cohorts, HIV patients on ART with suppressed viral loads and CD4 counts above 500 cells per mm^3 experience similar rates of chronic diseases as the general

population[122,123]. Furthermore, duration of HIV infection does not appear to be associated with an accelerated occurrence of co-morbidities[124].

Multiple studies have observed an increased risk of chronic non-AIDS conditions in HIV-positive patients in comparison to HIV-negative patients as well as high rates of co-morbidities at all ages. HIV patients present geriatric syndromes such as falls, sensory deficits and neurocognitive impairment as well as frailty earlier than uninfected individuals[124]. Approximately 50% of all HIV-positive individuals develop HIV-associated neurocognitive disorders (HAND) including myelopathy, peripheral neuropathy and dementia. However, most patients are asymptomatic while up to 12% have mild and 2% have severe disorders[114]. Incidence of chronic renal disease is increased at all ages in comparison to uninfected individuals with risk factors such as low CD4 count, high viral loads and use of certain ART (Tenofovir)[124]. Risk of chronic cardiovascular diseases including coronary artery disease, congestive heart failure and ischemic stroke with a 1.17 times increased risk of stroke and 1.5 times increased risk of acute myocardial infection at all ages[125,126]. Prevalence of osteoporosis and fracture is increased in comparison to the general population with a 3-fold increase in risk of fracture[127].

An epigenetic clock using CpG DNA methylation signatures has demonstrated accelerated aging in blood of HIV-positive patients being treated with ART and South African adolescents with perinatally acquired HIV (PHIV)[127]. Extrinsic epigenetic age acceleration was associated with HIV infection in the cohort of PHIV adolescents which is negatively correlated with cognitive functioning measures such as working memory, processing speed and executive functioning[127].

1.3.2 Telomere Attrition in HIV

Aging is a time-related deterioration of physiological integrity that eventually leads to impaired function and death. As summarized by López-Otin et al, the nine hallmarks of aging are genomic instability (such as DNA methylation), telomere shortening, mitochondrial dysfunction, cellular senescence, epigenetic alterations, loss of proteostasis, stem cell exhaustion, deregulated nutrient sensing and altered intercellular communication[128]. In this study, telomere attrition was used as a marker of aging in ART-treated HIV-positive and HIV-negative human lung and gut tissues.

Telomeres are repetitive nucleotide sequences (TTAGGG tandem repeats) located on the ends of each chromosome to preserve chromosome stability and prevent contact with neighbouring chromosomes. At birth, telomeres range from 5,000 to 15,000 base pairs and shorten with each round of cell division by 25 to 200 base pairs[129,130]. This limits the proliferation of human cells by inducing replicative senescence, differentiation or apoptosis. Telomere integrity depends on length of telomere and catalytic activity of enzyme telomerase and may also be disrupted by a variety of psychosocial, environmental and behavioural factors[131].

Multiple studies have examined telomere length in HIV infection. Liu et al demonstrated that mean absolute telomere length (aTL) in peripheral leukocytes of HIV-infected individuals was 27 kilobase pairs per genome shorter than the mean aTL of uninfected individuals. Slopes of aTL versus age were not different between HIV-infected and uninfected individuals. Active hepatitis C virus infection, smoking, worse CT emphysema severity score and reduced FEV1 during HIV infection have all been associated with shorter telomere length[132]. Pathai et al also

demonstrated significantly shorter telomeres in peripheral blood leukocytes of HIV-infected individuals compared to HIV-seronegative individuals in a South African cohort[133]. In small airway epithelium, Xu et al showed that telomere length was significantly decreased in patients living with HIV (PLWH) in comparison to HIV-negative patients with adjustments for age, sex and smoking pack-years[134]. Leung et al observed telomere shortening and methylation changes in peripheral blood during the short term period immediately following HIV seroconversion but not between post-HIV seroconversion and a later follow-up time point[135]. Shortening of telomere length in peripheral blood after HIV seroconversion was also demonstrated by Gonzalez-Serna et al[136]. From current literature, accelerated telomere length shortening seems to occur immediately after HIV infection but not during HIV infection.

Chapter 2: Experimental Approach

2.1 Working Hypothesis

The working hypothesis is that ART-treated HIV infection leads to shifts in the compositions of microbiomes in the gut-lung axis and these shifts are associated with changes in host response such as CD4 count, viral load and telomere length.

2.1.1 Specific Aims

To test the hypothesis, experiments were designed to address the following specific aims:

1) Quantify total bacterial population in the lung and small intestine tissue of HIV and non-HIV donors
2) Analyze the effects of HIV infection on the microbiome of lung and small intestine
3) Compare lung and small intestine microbiomes to host characteristics such as telomere length, CD4 count and viral load

Chapter 3: Methods

3.1 Introduction (Cohort)

HIV-positive and HIV-negative human lung and gut tissue samples were obtained from autopsies through the National NeuroAIDS Tissue Consortium (NNTC). Established in 1998, the NNTC collects, stores and distributes samples of central and peripheral nervous system tissue, blood, lung, small intestine and other organs from HIV-positive and negative patients. The NNTC is funded by the National Institute of Mental Health (NIMH) and the National Institute of Neurological Disorders and Stroke (NINDS) to support researchers conducting HIV research. The consortium is composed of four clinical sites: University of Texas (Galveston), University of California San Diego (UCSD), University of California Los Angeles (UCLA) and the Mount Sinai Medical Center (New York). For this study, samples originated from UCLA, Mount Sinai and Texas. Donors were HIV-positive patients previously on ART and HIV-negative patients who had expressed consent for tissue to be used for research purposes. To protect patient privacy, precautions were taken by utilizing unique identifiers for each donor. Procedures detailed by the NNTC were followed for extracting, characterizing, processing and storing tissue post-mortem. Clinical data including HIV status, age at death, gender, organ freeze time, medical history, $CD4^+$ count, viral load and lung and gut pathology was provided by the NNTC.

Clinical Site	Lung		Small Intestine	
	HIV +	HIV -	HIV +	HIV -
University of California Los Angeles	24	17	17	10
Mount Sinai Medical Center	3	4	3	4
University of Texas	2	--	2	--

Table 1. Summary of lung and small intestine samples by clinical site.

	HIV Positive	HIV Negative	p-Value
Subjects	29	19	--
Age at Death *(yrs)*	49.6 ± 9.2	61.5 ± 13.5	0.002
Gender (M:F)	23 : 6	6 : 13	0.012
Organ Freeze Time *(hrs)*	8.1 ± 7.4	5.7 ± 3.7	0.124
$CD4^+$ T cells *(cells/mm^3)*	163.9 ± 213.6	--	--
Detectable Viral Load (%)	73.1	--	--
Viral Load *(copies/mL)*	286473 ± 856709	--	--

Table 2. Summary of study cohort demographics. Statistical analysis performed using student t-test on age at death and organ freeze time and chi-squared test on gender.

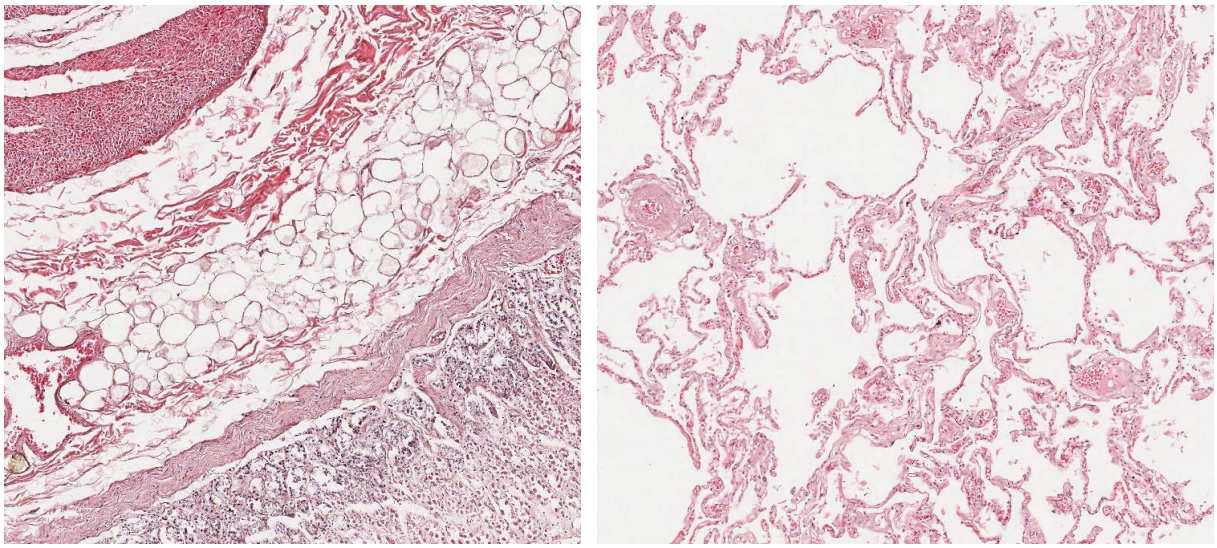

Figure 1. Histology of small intestine (left) and lung (right) from cohort.

3.2 Study Design

In this study, DNA was extracted from lung and gut tissue to capture both topical and trans-epithelial microbial composition. Using lung tissue helps reduce the possibility of contamination by fluids from the oral and nasal passages. An advantage in using tissue to

characterize the microbiome is the ability to measure tissue response in the same DNA sample. 54 samples from NNTC were initially used in the study and underwent DNA extraction. NanoDrop and Quant-iT dsDNA high sensitivity assay were then used to determine DNA quality and quantity respectively. After verifying the DNA samples were of satisfactory quality, the samples were diluted separately to the appropriate concentrations or dilution factors for 16S DNA ddPCR, telomere qPCR and 16S DNA MiSeq.

The first experiment of the study involved quantifying the 16S rRNA gene using ddPCR to determine bacterial load. This also gave an idea of what sequence counts could be expected after MiSeq sequencing. Samples were sent to the University of British Columbia Sequencing and Bioinformatics Consortium after library preparation, validation and dilution was completed. From the data generated by MiSeq, alpha, beta diversities and prominence of specific bacteria in experimental groups were investigated using Quantitative Insights Into Microbial Ecology (QIIME2) and various packages from R including phyloseq and vegan[136]. Absolute telomere length was measured using qPCR to investigate changes in cellular senescence in HIV-positive donors in comparison to HIV-negative donors and whether telomere length could be associated with different microbial compositions.

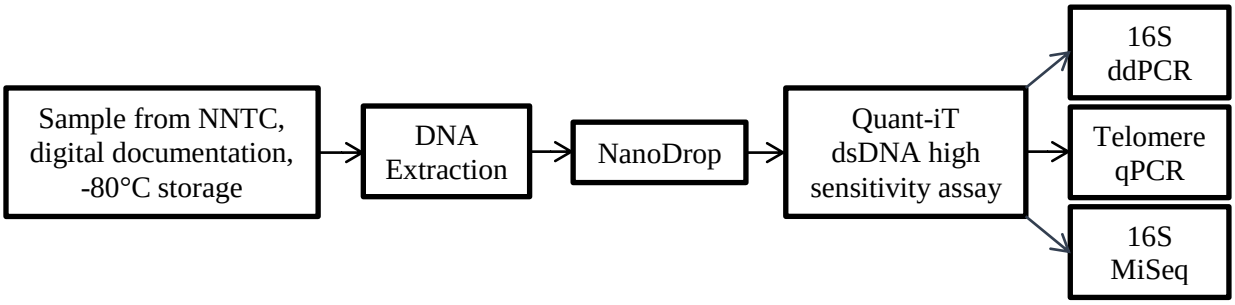

Figure 2. Experimental workflow of study.

3.2.1 16S rRNA Gene

16S ribosomal RNA is a component of the 30S small subunit of prokaryotic ribosomes and is present in all bacteria. The 16S rRNA gene is widely used in the study of bacteria and microbiomes as it contains nine hypervariable regions (V1 to V9) and conserved regions in between the hypervariable regions. The nine hypervariable regions can help differentiate between bacteria from the phylum to genus levels and in some cases even the species level can be identified. The conserved regions can be used as a target for PCR primers to amplify various combinations of the variable regions for quantitative and qualitative purposes such as investigating bacterial load and microbial community composition. Several databases of 16S rRNA gene sequences exist and this study used the SILVA database to align and classify sequences.

3.3 DNA Extraction and Storage (NNTC Tissue, numbering)

After receiving tissue samples from the NNTC, samples were documented digitally and stored in the -80°C freezer. Lung and gut tissue samples were cut in the biosafety cabinet on a clean plastic surface on dry ice to maintain sample integrity and to ensure samples were kept frozen. Instruments used to excise tissue as well as excision platforms were cleaned with ethanol followed by Cavicide™ (general viral and bacterial decontaminant) after each sample. Approximately 60 mg of sample tissue was cut from each sample, weighed by analytical balance and placed into a previously prepared clean 2 mL screw top micro tube with a single metal bead.

DNA extraction was performed following the user-developed protocol “Purification of total DNA from soft tissues using the TissueLyser and the DNeasy® Blood & Tissue Kit found through Qiagen® (Maryland, USA) with the following exceptions. Tissue homogenization (step

4) was performed using the “Purification of DNA from Animal and Human Tissues” protocol (pages 23 to 24) from the Qiagen® TissueLyser LT Handbook (May 2009). Incubation at 56°C in a shaker incubator was performed overnight, 4 µL of RNase (100 mg/mL) was added after 56°C overnight incubation and 100 µL of AE buffer (elution buffer comprised of 10 mM Tris-Cl and 0.5 mM EDTA; pH 9.0 from Qiagen®) was used to elute all samples. Extraction negative controls were included in the tissue extraction process to account for potential contamination in disposables and reagents.

After DNA extraction, NanoDrop (Delaware, USA) was utilized to determine quality and estimate quantity through the use of optical density (OD) 260/280, OD 260/230 and OD 260 measurements. The 260/280 ratio is used to assess purity of nucleic acids with a ratio of approximately 1.8 being accepted as “pure” DNA. The 260/230 ratio is a secondary measure of nucleic acid purity with values typically in the 2.0 to 2.2 range. OD 260 is used to determine the quantity of nucleic acid in a sample. DNA concentration were determined using Quant-iT™ dsDNA High-Sensitivity Assay Kit (Thermo Fisher Scientific, Massachusetts, USA) and comparing samples to a standard curve after measuring fluorescence at 485/530 nm.

All samples were placed into 4°C after DNA extraction to avoid repeated freeze and thaw cycles. After completion of MiSeq library preparation, 16S droplet digital polymerase chain reaction (ddPCR) and telomere quantitative polymerase chain reaction (qPCR) samples were organized and placed into -80°C freezer for long-term storage.

3.4 Experiment 1: Bacterial Load

3.4.1 ddPCR Theory and Conditions

Droplet digital PCR was used to examine bacterial load in samples. Small intestine DNA samples were sequentially diluted to 1:1000 and lung DNA samples were diluted 1:50. Prior to droplet formation, the PCR reaction volume was 20 µL with the following components: 10 µL of BioRad 2x QX200™ ddPCR™ EvaGreen® Supermix, 0.2 µL of 10 µM 16S forward primer (63F), 0.2 µL of 10 µM 16S reverse primer (355R), 7.6 µL DNase/RNase free water and 2 µL DNA template. Using the QX200™ Droplet Generator, 70 µL of droplet generation oil was dispensed into the DG8 droplet generator cartridges along with 20 µL of PCR reaction in separate wells. The sample is then partitioned into approximately 20,000 nano-liter sized droplets using water-oil emulsion with a final volume of 40 µL. All samples including plate controls, water negative and extraction negatives were run in duplicate. The plate is then sealed with PCR foil at 180 °C and then placed into the Bio-Rad MyCycler Thermal Cycler to amplify the 16S region according to the following conditions:

1 x (5 minutes at 95°C)

40 x (30 seconds at 95°C, 1 minute at 60°C)

Ramp rate 2°C/second between temperature changes

1 x (5 minutes at 4°C)

1 x (5 minutes at 90°C)

The 16S rRNA gene V1-V2 region was amplified using universal 16S primers 63F and 355R.

Primer Name	**Primer Sequence (5' – 3')**
63F	GCAGGCCTAACACATGCAAGTC
355R	CTGCTGCCTCCCGTAGGAGT

Table 3. Forward and reverse primer sequences used in 16S rRNA ddPCR.

During PCR, the inactive form of EvaGreen was heat-activated into the active variation which forms a complex with hybridized DNA. After thermal cycling, samples were analyzed using the QX200™ Droplet Reader which analyzes each droplet individually using a binary detection system to differentiate between PCR-positive and PCR-negative droplets based on fluorescence. Determining the amount of PCR-positive droplets then allows the absolute quantification of 16S DNA template concentration in the original sample.

3.4.2 ddPCR Data Analysis

The QX200™ Droplet Reader reads approximately 12,000 to 16,000 droplets and connects to the QuantaSoft™ Software which was used for assembling plate layout and data acquisition. Quality control was performed by ensuring that the droplet count was above 12,000 for each sample and observing a clear separation in fluorescence amplitude between PCR-positive and PCR-negative droplets. Using a threshold of 10,000 fluorescent units to differentiate between PCR-positive and PCR-negative droplets, copies per microliter (µL) was generated through the software and further adjusted for dilution factor, plate differences and extraction negative. Previously determined DNA concentrations were then used to normalize the results to copies per nanogram of DNA to account for variation in initial DNA concentrations.

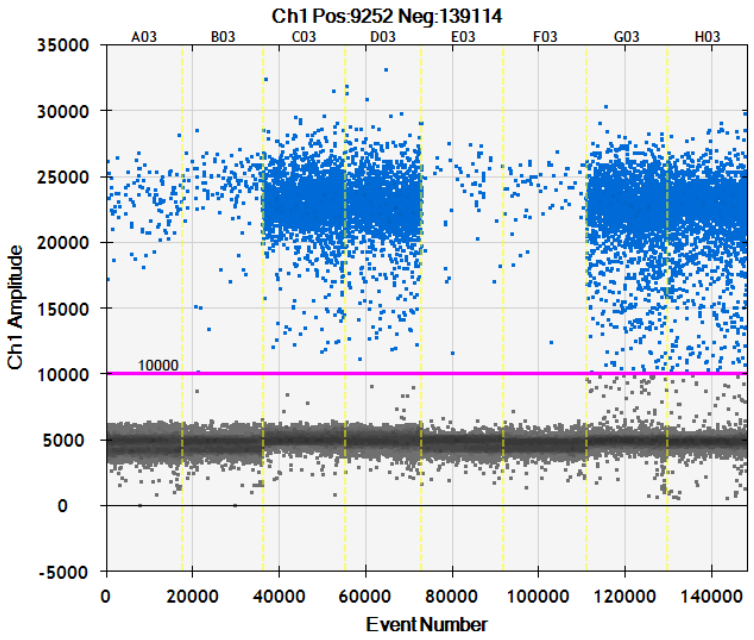

Figure 3. Example of fluorescence amplitude graph from QuantaSoft™ Software.

3.5 Experiment 2: Telomere qPCR

3.5.1 qPCR Theory and Conditions

Quantitative PCR was used to determine absolute telomere length in lung and small intestine DNA samples using the protocol described by O'Callaghan and Fenech (2011)[137]. Samples were diluted to 5 ng/µL excluding those that had initial concentrations below 5 ng/µL. The final qPCR reaction volume was 20 µL and included the following: 10 µL 2 x Bio-Rad iTaq™ Universal SYBR® Green Supermix, 1µL of 2 µM forward primer, 1 µL of 2 µM reverse primer, 4 µL RNase free water and 4 µL DNA template at 5 ng/µL. Samples with concentrations below 5 ng/µL were added individually with adjustment of water volume so that total DNA amount was 20 ng in each reaction.

Primer Name	Species	Primer Sequence (5' – 3')
teloF	Human/rodent	CGGTTTGTTTGGGTTTGGGTTTGGGTTTGGGTTTGGGTT
teloR	Human/rodent	GGCTTGCCTTACCCTTACCCTTACCCTTACCCTTACCCT
36B4F	Human	CAGCAAGTGGGAAGGTGTAATCC
36B4R	Human	CCCATTCTATCATCAACGGGTACAA

Table 4. Telomere and 36B4 primers.

For the telomere standard, a 10-fold serial dilution of 1 ng/µL stock telomere concentration was performed with 8 standard points and the first point starting at the 1:10 dilution. The single copy gene standard used was 36B4 which encodes the acidic ribosomal phosphoprotein P0 (RPLP0) and was used to determine genome copies per sample. For the 36B4 standard, a 4-fold serial dilution of 40 pg/µL stock 36B4 concentration was performed with 8 standard points and the first point starting at the 1:16 dilution.

Standard sequences and absolute telomere qPCR standards kB calculations shown below:

Telomere standard 84 bp: (TTAGGG)[14]

36B4 standard 75 bp: CAGCAAGTGGGAAGGTGTAATCCGTCTCCACAGACAAGGCCAG GACTCGTTTGTACCCGTTGATGATAGAATGGG

Telomere standard starting concentration: 1 ng/µL (use 4 ng/reaction)

$$\frac{4 \times 10^{-9} g}{0.44 \times 10^{-19} g\ (telomere\ oligomer\ weight)}$$

$$= 9.09 \times 10^{10} (molecules\ of\ telomere\ oligomer) \times 84\ (oligomer\ length)$$

$$= 7.64 \times 10^{9} kB$$

36B4 standard starting concentration: 4 pg/µL (use 16 pg/reaction)

$$\frac{16 \times 10^{-12} g}{0.38 \times 10^{-19} g\ (36B4\ oligomer\ weight)} = \frac{4.211 \times 10^{8} (molecules\ of\ 36B4\ oligomer)}{2\ (diploid\ copies)}$$

$$= 2.11 \times 10^{8} diploid\ copies$$

Telomere Standard		
Dilution	Concentration	kB
Stock	1 ng/uL	7.636E+09
1:10	0.1 ng/uL	7.636E+08
1:100	10 pg/uL	7.636E+07
1:1000	1 pg/uL	7.636E+06
1:10000	0.1 pg/uL	7.636E+05
1:100,000	10 fg/uL	7.636E+04
1:1,000,000	1 fg/uL	7.636E+03
1:10,000,000	0.1 fg/uL	7.636E+02
1:100,000,000	10 ag/uL	7.636E+01

36B4 Standard		
Dilution	Concentration	kB
Stock	4 pg/uL	2.11E+08
1:4	1 pg/uL	5.26E+07
1:16	250 fg/uL	1.32E+07
1:64	62.5 fg/uL	3.29E+06
1:256	15.625 fg/uL	8.22E+05
1:1,024	3.906 fg/uL	2.06E+05
1:4,096	976.5 ag/uL	5.14E+04
1:16,384	244.1 ag/uL	1.28E+04
1:65,536	61.035 ag/uL	3.21E+03
1:262,144	15.259 ag/uL	8.03E+02

Table 5. Telomere and 36B4 standard curve concentrations. Eight standard points were used in both telomere (1:10 dilution to 1:100,000,000 dilution) and single copy gene 36B4 (1:16 dilution to 1:262,144 dilution) standards.

Samples were run in triplicate using telomere and 36B4 primers separately on the same 384-well plate. Positive controls included K562 (human chronic myelogenous leukemia cell line) DNA, HEK293 (human embryonic kidney cell line) DNA and two human controls extracted from buffy coat. RNase free water was used as no template control. qPCR was run on Bio-Rad CFX96 Touch™ Real-Time PCR Detection System according to the following conditions:

1 x (10 minutes at 95°C)

40 x (15 seconds at 95°C, 1 minute at 60°C)

Melt curve

Quality control was performed by ensuring that standard curves had at least 5 points, an efficiency value between the range of 90% to 110%, an R-squared value of above 0.98 and the

no template control had a quantitation cycle (Cq) value above 30. All measurements had to be within range of the standard curve and Cq standard deviations less than 1.000 between triplicates.

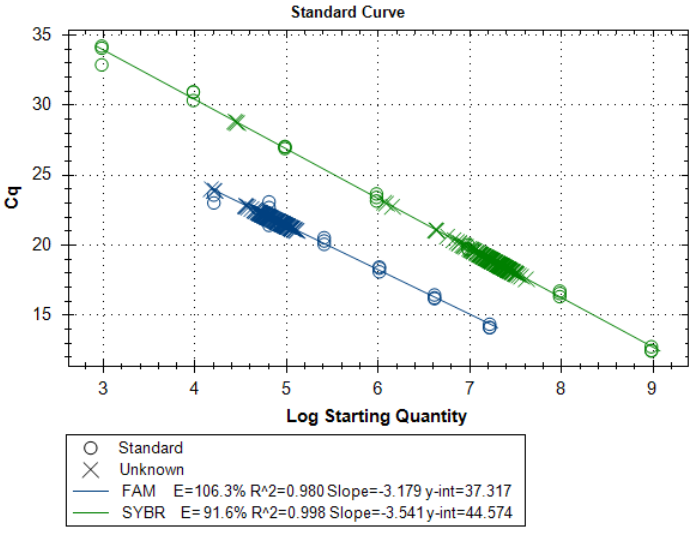

Figure 4. Example of experimental run to measure absolute telomere length using qPCR.

3.5.2 qPCR Telomere Data Analysis

Starting quantity (SQ) of both telomere and 36B4 were calculated from the standard curve and Cq values. Absolute telomere length (aTL) was then calculated using the following method:

$$\frac{SQ\ Telomere}{SQ\ 36B4} = kB/SCG$$

$$\frac{Total\ length\ (kB/SCG)}{92\ (number\ of\ telomeres\ in\ 23\ pairs\ of\ chromosomes)} = length\ per\ telomere\ (kB)$$

To correct for plate-to-plate variability, positive controls were run on each plate and the ratios between plates were used to normalize aTL results.

3.6 Experiment 3: Illumina Miseq Sequencing

3.6.1 MiSeq Sequencing Platform

The Illumina MiSeq next generation sequencer was used to characterize bacterial community composition in the lung and small intestine tissue of HIV-positive and HIV-negative donors. The Illumina NGS workflow consisted of four basic steps: library preparation, cluster generation, sequencing and data analysis. Library preparation, which will be detailed in the next section, consisted of amplifying the target of interest and labeling the individual samples with unique barcode combinations and adapter fragments to allow for high-throughput. Cluster generation involved loading the library into a flow cell, ligation of library adaptors to complementary surface-bound oligos and bridge amplification of bound fragments into distinct, clonal clusters.

Illumina uses sequencing by synthesis technology in which four fluorescently-labeled nucleotides are used to sequence the clonal clusters on the flow cell surface. In a single sequencing cycle, a labeled deoxyribonucleotide triphosphate (dNTP) with a reversible terminator was added onto the end of the nucleic acid chain. The reversible terminator inhibited polymerization which allowed the fluorescent dye to be imaged after each cycle to identify the base by different colours of fluorescence. The terminator was then enzymatically cleaved to permit incorporation of the subsequent dNTP. This cycle was then repeated for 250 cycles to fully sequence the forward and reverse reads amplified during library preparation. QIIME2, a next-generation microbiome bioinformatics platform and SILVA, an rRNA database were then used for processing, alignment and sequence quality control. Further data analysis was performed using packages phyloseq and vegan in R studio.

3.6.2 Library Preparation

MiSeq library preparation was performed by adapting the Schloss laboratory dual-index sequencing protocol published by Kozich et al[138]. The V4 region of the 16S rRNA gene was used as the target for MiSeq sequencing of the microbiome. After DNA extraction of samples, touchdown PCR was used to amplify the target gene and attach sequence identifiers and adaptors. The touchdown technique was chosen to increase specificity by starting at an annealing temperature higher than the optimal and gradually decreasing the temperature in subsequent cycles. At temperatures higher than the calculated optimal temperature, the primer and template bind more specifically. As the temperature gradually lowers in subsequent cycles, annealing of primer to template becomes less specific but more frequent allowing increased amplification of amplicons created in the earlier high-temperature cycles.

The final touchdown PCR reaction volume was 20 µL and included the following: 2 µL of 10x Buffer II, 0.15 µL of AccuPrime Taq Polymerase, 2 µL of 10µM reverse and forward primer combination, and a combined 15.85 µL of extracted DNA sample and RNase free water adjusted for an input of 20 ng of DNA due to varying concentrations of extracted DNA. Touchdown PCR was run on the Bio-Rad Mycycler Thermal Cycler using the following conditions adapted from a protocol by Korbie & Mattick:

1 x (2 minutes at 95°C)

20 x (20 seconds at 95°C, 15 seconds at 60°C/54°C, 90 seconds at 72 °C)

Temperature decrease of 0.3°C at each cycle from 60°C to 54°C

20 x (20 seconds at 95°C, 15 seconds at 55°C, 90 seconds at 72 °C)

1 x (5 minutes at 72°C)

The samples are run along with a negative control (water) and positive control (mock community). Final product including adaptor, barcode, pad, link, primer and target sequence was approximately 400 base pairs with the target sequence being 250 base pairs long.

	Forward Primers (5' to 3')
SA501	AATGATACGGCGACCACCGAGATCTACACATCGTACGTATGGTAATTGTGTGCCAGCMGCCGCGGTAA
SA502	AATGATACGGCGACCACCGAGATCTACACACTATCTGTATGGTAATTGTGTGCCAGCMGCCGCGGTAA
SA503	AATGATACGGCGACCACCGAGATCTACACTAGCGAGTTATGGTAATTGTGTGCCAGCMGCCGCGGTAA
SA504	AATGATACGGCGACCACCGAGATCTACACCTGCGTGTTATGGTAATTGTGTGCCAGCMGCCGCGGTAA
SA505	AATGATACGGCGACCACCGAGATCTACACTCATCGAGTATGGTAATTGTGTGCCAGCMGCCGCGGTAA
SA506	AATGATACGGCGACCACCGAGATCTACACCGTGAGTGTATGGTAATTGTGTGCCAGCMGCCGCGGTAA
SA507	AATGATACGGCGACCACCGAGATCTACACGGATATCTTATGGTAATTGTGTGCCAGCMGCCGCGGTAA
SA508	AATGATACGGCGACCACCGAGATCTACACGACACCGTTATGGTAATTGTGTGCCAGCMGCCGCGGTAA

Table 6. List of forward sequencing primers adapted from the Schloss Lab (Adaptor, Barcode, Pad, Link and Primer).

	Reverse Primers (3' to 5')
SB701	CAAGCAGAAGACGGCATACGAGATAAGTCGAGAGTCAGTCAGCCGGACTACHVGGGTWTCTAAT
SB702	CAAGCAGAAGACGGCATACGAGATATACTTCGAGTCAGTCAGCCGGACTACHVGGGTWTCTAAT
SB703	CAAGCAGAAGACGGCATACGAGATAGCTGCTAAGTCAGTCAGCCGGACTACHVGGGTWTCTAAT
SB704	CAAGCAGAAGACGGCATACGAGATCATAGAGAAGTCAGTCAGCCGGACTACHVGGGTWTCTAAT
SB705	CAAGCAGAAGACGGCATACGAGATCGTAGATCAGTCAGTCAGCCGGACTACHVGGGTWTCTAAT
SB706	CAAGCAGAAGACGGCATACGAGATCTCGTTACAGTCAGTCAGCCGGACTACHVGGGTWTCTAAT
SB707	CAAGCAGAAGACGGCATACGAGATGCGCACGTAGTCAGTCAGCCGGACTACHVGGGTWTCTAAT
SB708	CAAGCAGAAGACGGCATACGAGATGGTACTATAGTCAGTCAGCCGGACTACHVGGGTWTCTAAT
SB709	CAAGCAGAAGACGGCATACGAGATGTATACGCAGTCAGTCAGCCGGACTACHVGGGTWTCTAAT
SB710	CAAGCAGAAGACGGCATACGAGATTACGAGCAAGTCAGTCAGCCGGACTACHVGGGTWTCTAAT
SB711	CAAGCAGAAGACGGCATACGAGATTCAGCGTTAGTCAGTCAGCCGGACTACHVGGGTWTCTAAT
SB712	CAAGCAGAAGACGGCATACGAGATTCGCTACGAGTCAGTCAGCCGGACTACHVGGGTWTCTAAT

Table 7. List of reverse sequencing primers adapted from the Schloss Lab (Adaptor, Barcode, Pad, Link and Primer).

All samples then underwent 1.5% agarose gel electrophoresis to check that the target amplicon was successfully amplified and no additional bands were present.

Ladder fr44 fr45 fr46 fr47 fr48 fr49 fr50 fr51 fr52 fr53 fr54 fr55 fr56 fr57

Figure 5. Example of 1.5% agarose gel ran to visual PCR product with 100 base pair (bp) DNA ladder.

The Invitrogen SequalPrep Plate Normalization Kit was then used for library clean up and normalization of all samples to 5 ng. AMPure XP system magnetic beads (Beckman Coulter, Brea, California) were used to clean up the library sample by removing nucleotides, primers, and components that were not the target amplicon. Quality control was performed using the DNA 1000 assay and Agilent Bioanalyzer 2100 (Agilent Technologies Inc, Santa Clara, CA, USA) to determine whether the amplicon was the correct size, sample purity and approximate concentration.

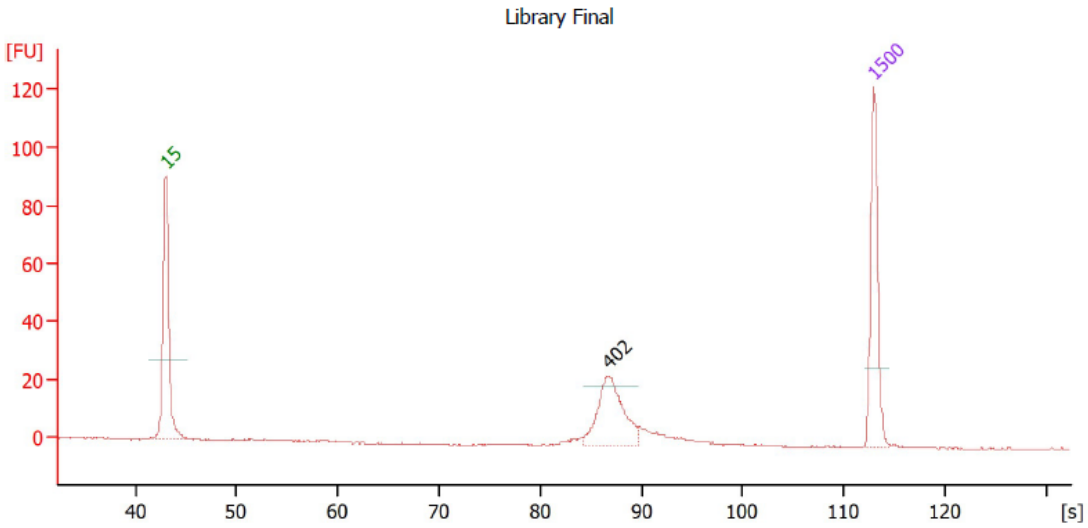

Overall Results for sample 1 : **Library Final**

Number of peaks found: 1

Peak table for sample 1 : **Library Final**

Peak	Size [bp]	Conc. [ng/µl]	Molarity [nmol/l]	Observations
1	15	4.20	424.2	Lower Marker
2	402	1.92	7.2	
3	1,500	2.10	2.1	Upper Marker

Figure 6. DNA 1000 Assay on Agilent Bioanalyzer 2100 to check for amplicon size, sample purity and concentration.

Actual concentration was measured by Quant-iT dsDNA high sensitivity assay and then diluted to 4 µM with 9.0 pH TE buffer. The prepared sample was then sent for Illumina MiSeq sequencing (Illumina, Redwood City, California) with 2 x 250 paired end read chemistry at the UBC Sequencing and Bioinformatics Consortium by Dr. Sunita Sunha.

3.6.3 QIIME2 16S Sequencing Data Analysis

16S sequencing data was analysed using next-generation microbiome bioinformatics platform QIIME 2™ (2018.4) for clean-up of raw sequencing data. Raw sequencing data was imported as fastq.gz files and sequence quality control and feature table construction were

completed using the Divisive Amplicon Denoising Algorithm 2 (DADA2) QIIME 2 plugin. The DADA2 pipeline detects and corrects sequence data and filters out PhiX and chimeric sequences. PhiX was used as a control library to provide quality control for cluster generation and sequencing for the Illumina MiSeq run. Chimeric sequences are artifacts created during PCR and contain DNA from two or more parent sequences. When an amplicon terminates prematurely, it may be extended again in a subsequent cycle if another DNA strand with a similar starting region attaches onto the existing amplicon. Chimeric sequences can lead to the false "discovery" of novel organisms and are removed during sequence quality control.

Sequences were aligned to the SILVA database (version) for identification of bacteria based on 16S. All samples were subsampled to 2486 sequence reads for further analysis in R studio (version 1.1.453, R version 3.5.0) using packages phyloseq (version 1.25.2) and vegan (version 2.5-2) to determine alpha and beta diversities. Alpha diversity was measured by richness (total number of features), evenness (similarity in numbers of individual features) and Shannon diversity index which accounts for both richness and evenness. Beta diversity was measured using a principal coordinates analysis of weighted Unifrac distances. Distribution of features at the phylum and genus taxonomic levels and comparison of relative abundance in specific phyla and genera was investigated.

3.7 Troubleshooting

As previously mentioned, this study originally consisted of 54 samples from the NNTC cohort. After completion of 16S ddPCR, qPCR telomere and 16S MiSeq, a request for additional samples was made to the NNTC and 32 more samples were processed for analysis. The initial 54

samples were re-extracted to reduce batch effect and all samples went through the same pipeline of experiments as previously mentioned.

One limitation of the study was that the NNTC performed the autopsies and therefore there was no method to define where specifically in the lung and small intestine the tissues are from. The lung tissue may have originated from different areas and may therefore have differences in microbial composition as shown through previous studies on locations differing in microbial composition in the lung. Another limitation was the inability to control organ freeze time and potential contaminants from autopsy using negative controls such as instrument washes.

3.7.1 Experiment 1: Bacterial Load

Experimental conditions for ddPCR were optimized through testing one sample each of high, medium and low DNA concentrations at different dilutions for both lung and small intestine samples. 1:1000 dilution (through 1:10 serial dilutions) for small intestine samples and 1:50 dilution for lung samples were determined to be the optimal settings for sufficient separation of PCR-positive and PCR-negative droplets.

3.7.2 Experiment 2: qPCR Telomere

Telomere and single copy gene 36B4 standard curve optimization tests were run prior to sample measurement to determine the optimal serial dilution and starting concentration. However, after comparing Cq values to earlier experiments, it was determined that the previous stock for telomere and 36B4 standards were underperforming which may have been due to DNA degradation from storage and freeze-thaw cycles. New stocks of telomere and 36B4 standards

(Integrated DNA Technologies, Coralville, Iowa) were ordered, reconstituted and aliquoted into working concentrations.

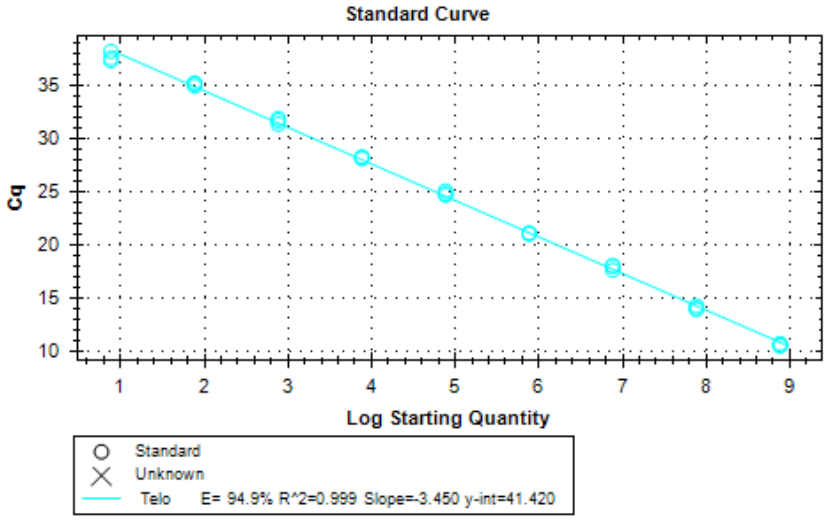

Figure 7. Telomere standard optimization

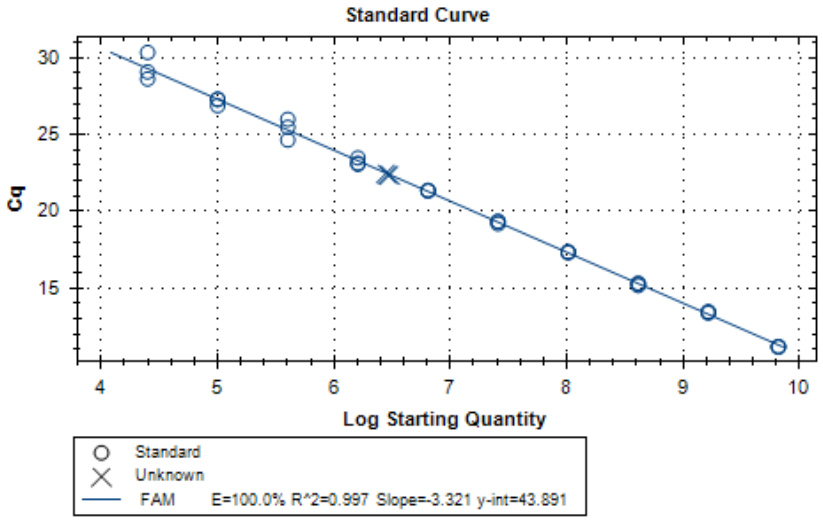

Figure 8. 36B4 standard optimization

3.7.3 Experiment 3: 16S MiSeq

Prior to the MiSeq library preparation method mentioned above, the "16S Metagenomic Sequencing Library Preparation" protocol from Illumina was used. This protocol amplified the V3V4 region of 16S and used 2 x 300 paired end read chemistry to sequence the prepared library. However, this resulted in a lower overlap of the paired end reads and increased error rates compared to previous studies (based on sequenced Mock community). Therefore, the Schloss laboratory MiSeq protocol amplifying the V4 regions was utilized for the final results. Experimental optimizations for library preparation included testing for optimal input DNA concentration for touchdown PCR and re-extracting samples with very low DNA concentrations in initial extractions.

Chapter 4: Results

4.1 Experiment 1: 16S Bacterial Load

Bacterial load was expressed as 16S copies amplified normalized to total nanograms of DNA measured on the ddPCR platform. For lung samples, there were 29 HIV-positive samples and 21 HIV-negative samples. For small intestine samples, there were 22 HIV-positive samples and 12 HIV-negative samples. Out of 14 HIV-negative small intestine samples, two samples were deemed to be outliers and removed from the analysis. A two-way analysis of variance (ANOVA) was applied in the figure below, demonstrating that HIV status did not have a significant effect on 16S bacterial load while location of sample (lung or small intestine) had a statistically significant effect.

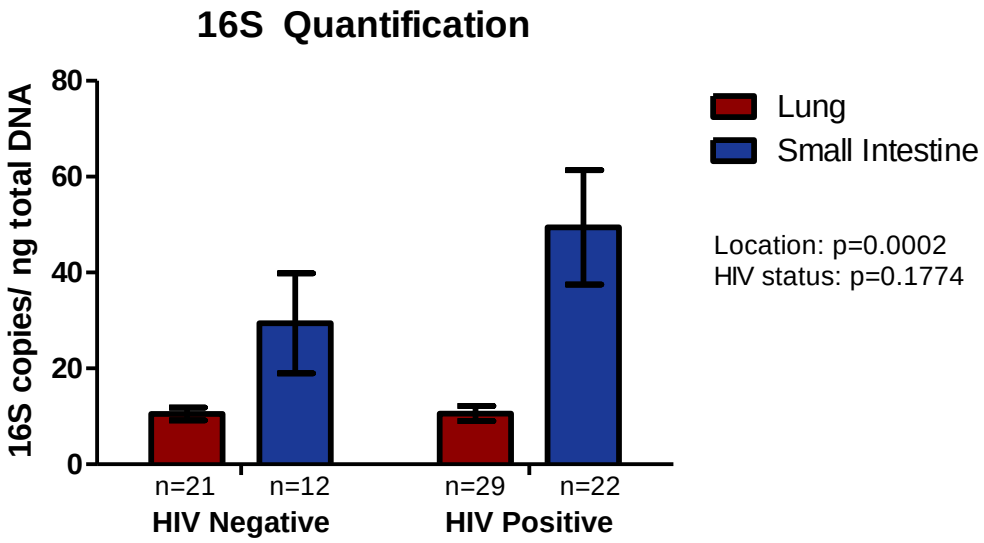

Figure 9. Bacterial load in lung and small intestine of HIV-positive and HIV-negative donors by 16S rRNA. Error bars represent standard error of mean. Statistical analysis completed using two-way ANOVA.

To determine whether 16S bacterial load in lung and small intestine were correlated, sample values measured by ddPCR were graphed on the x- and y-axis respectively. Two samples were omitted as outliers as previously mentioned. The figure below shows evidence of correlation between lung and small intestine 16S quantification (p=0.039) using a linear regression model.

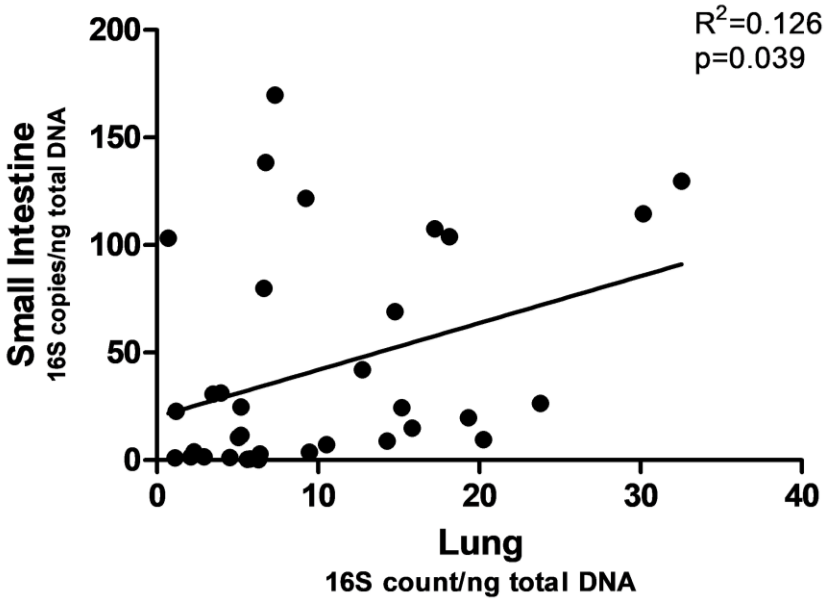

Figure 10. 16s rRNA bacterial load correlation between lung and small intestine samples. Statistical analysis completed using linear regression.

4.2 Experiment 2: Absolute Telomere Length

Absolute telomere length (aTL) was measured in kilobases per genome using qPCR targeting the telomere gene and normalizing to single copy gene (SCG) 36B4. In the lung, aTL was found to be significantly shorter in HIV-positive donors in comparison to HIV-negative donors (p=0.039) while aTL did not differ between HIV-positive and HIV-negative donors in the small intestine.

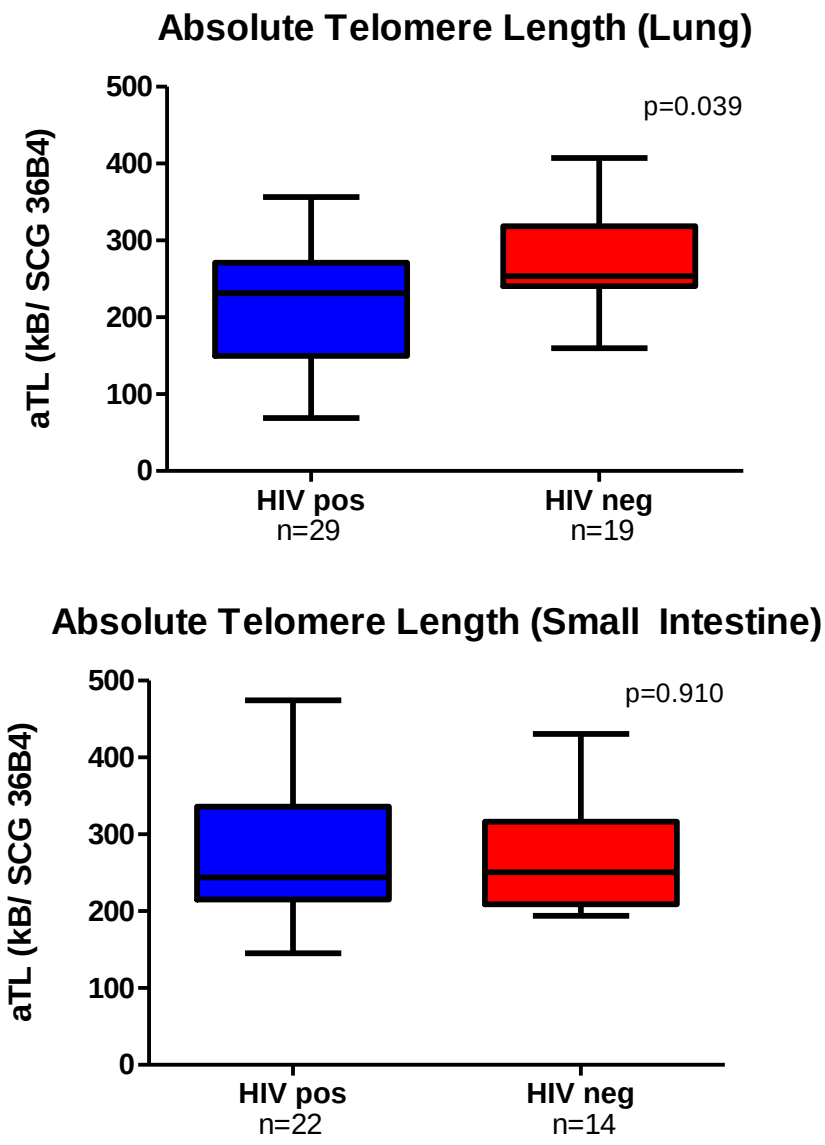

Figure 11. Comparison of absolute telomere length (kilobases per SCG 36B4) between HIV-positive and HIV-negative donors in lung and small intestine. Box extends from 25th to 75th percentiles and whiskers represent minimum to maximum values. Statistical analysis completed using Mann-Whitney test.

The effect of HIV status on the relationship between aTL and age was determined to be not significant in both the lung (p=0.449) and small intestine (p=0.066) using linear regression and analysis of covariance.

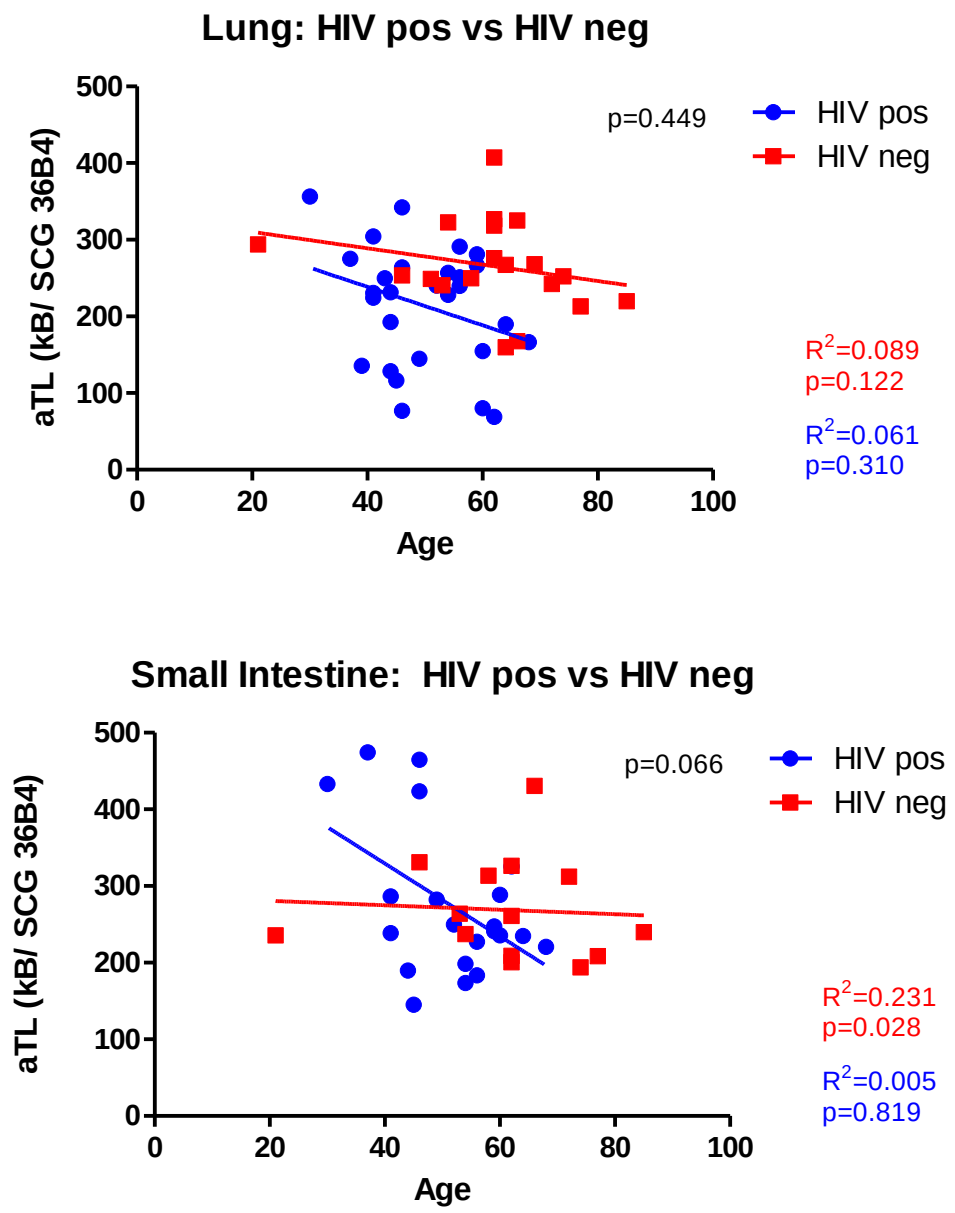

Figure 12. Effect of HIV status on relationship between aTL and age in lung and small intestine. Statistical analysis completed using linear regression on aTL and age and ANCOVA on difference between slopes generated from HIV-positive and HIV-negative donors.

There was no correlation between bacterial load and aTL in both lung and small intestine of HIV-positive and HIV-negative donors.

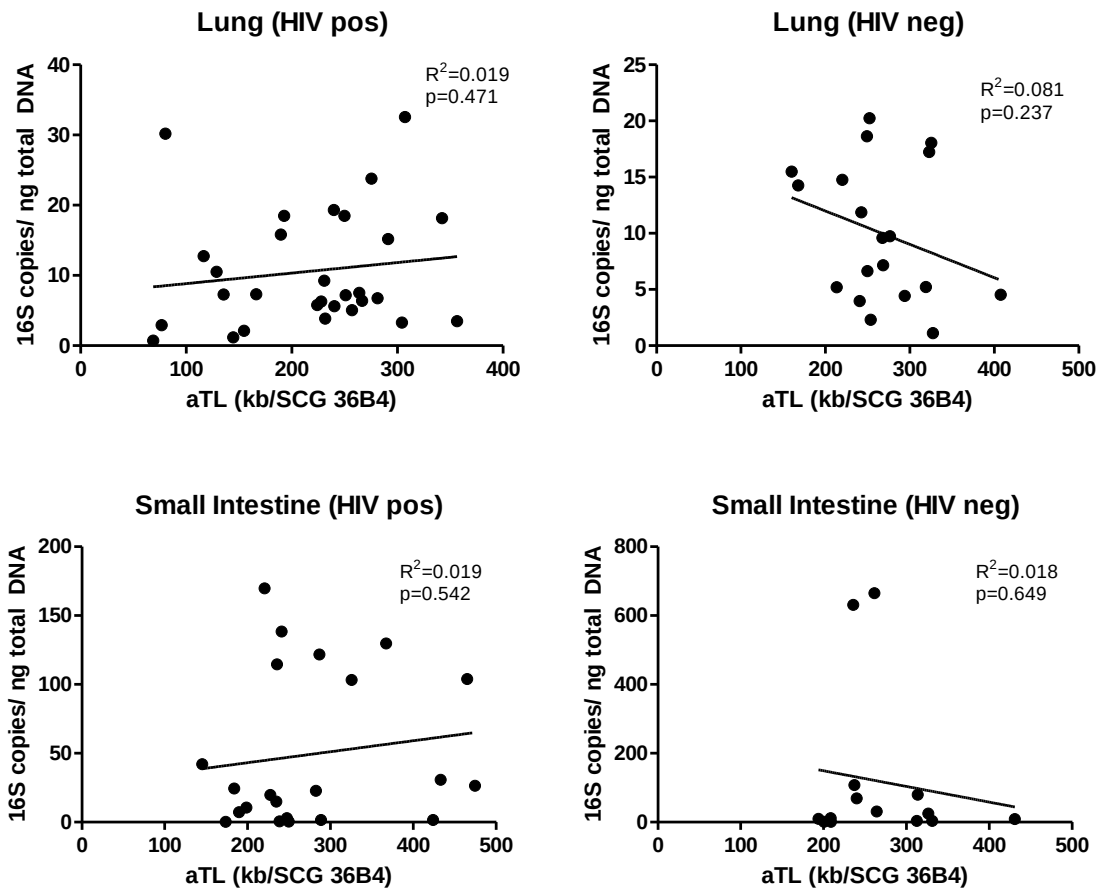

Figure 13. Correlation between 16S rRNA and aTL. Statistical analysis completed using linear regression.

4.3 Experiment 3: 16S MiSeq Sequencing

4.3.1 Lung

4.3.1.1 Lung Alpha and Beta Diversity

Alpha diversity measures of observed ASVs (number present), Shannon and Simpson indices were used to quantify diversity within individual lung samples. As previously mentioned ASVs are categorizations of sequences in QIIME2 and used to identify sequences through alignment with 16S databases. Shannon and Simpson indices are methods of calculating in-sample diversity by accounting for both number of species (richness) and distribution of species

(evenness). Microbiomes of HIV-positive and HIV-negative donors did not differ in terms of observed ASVs, Shannon index and Simpson index with p-values of 0.760, 0.401 and 0.401 respectively.

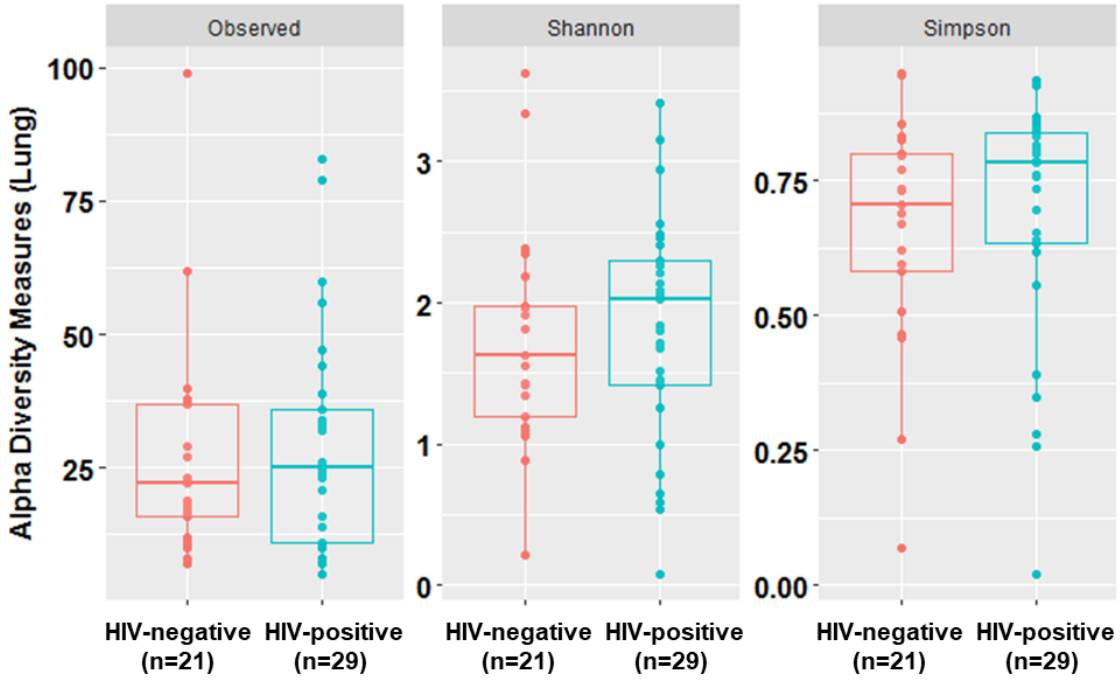

Figure 14. Alpha diversity measures comparing microbiota in lungs of HIV-positive to HIV-negative donors. Comparisons of observed ASVs, Shannon index and Simpson index yielded p-values of 0.760, 0.401 and 0.401 respectively. Statistical analysis completed using Wilcoxon rank sum test with continuity correction.

Beta diversity determines dissimilarities between individual samples using ordination methods to demonstrate differences in microbial composition visually. In this study, a principle coordinate analysis (PCoA) and weighted UniFrac methods were used to visualize the microbiome data. Principle coordinate analysis is a method to visualize dissimilarities using a distance matrix and assigns each sample a location in low-dimensional space. UniFrac is a distance matrix used to compare communities and incorporates information on phylogenetic distances between observed organisms. Weighted UniFrac incorporates abundances of ASVs,

diminishing the impact of low abundance features. In the lung, HIV-positive and HIV-negative microbial compositions were not different with a p-value of 0.799 using permutational multivariate analysis of variance (PERMANOVA).

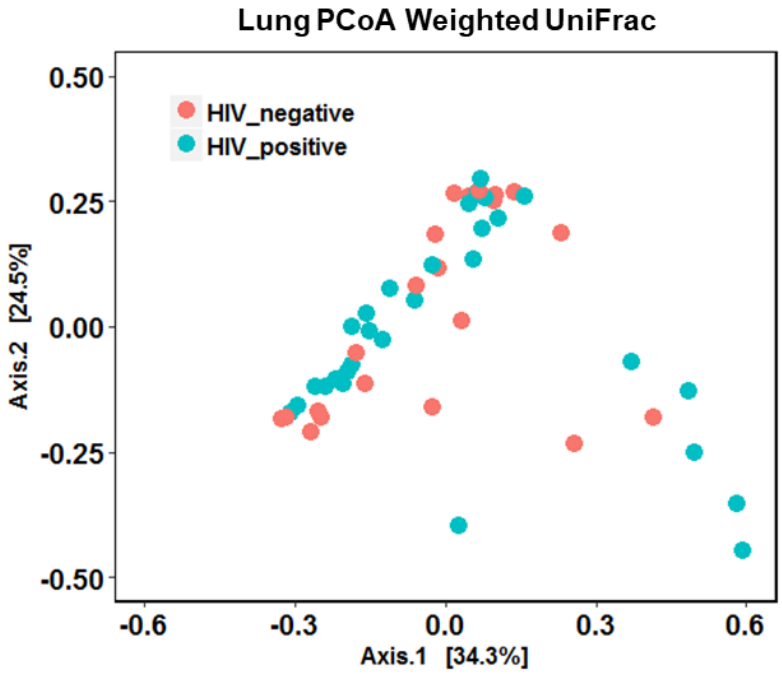

Figure 15. PCoA plot using weighted unifrac of microbial compositions in lung of HIV-positive and HIV-negative donors. Statistical analysis completed using PERMANOVA (p=0.799).

Further beta diversity analysis of microbial compositions based on telomere length, viral load, CD4 count and clinical site were performed. Telomere length was separated into two groups with samples over and less than 250 kilobases per genome which was chosen as it gave the most even separation of samples. Viral load was separated by samples with less than or more than 75 HIV copies per milliliter as this was the lowest detectable amount in this database. CD4 count was grouped by samples under and over 200 cells per mm^3 as patients with a CD4 count of under 200 cells per mm^3 are diagnosed with AIDS.

Microbial compositions did not differ based as telomere length, viral load, CD4 count and clinical site with PERMANOVA generated p-values of 0.987, 0.191, 0.903 and 0.228 respectively.

Figure a

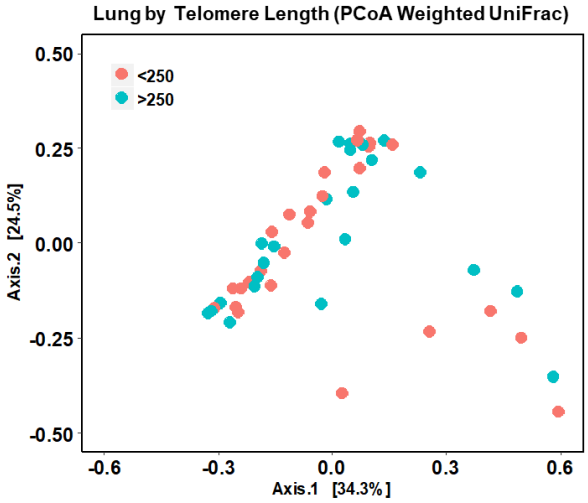

Figure b

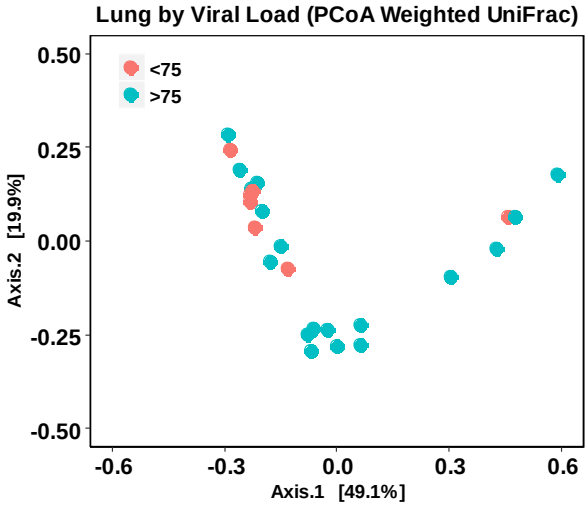

Figure c

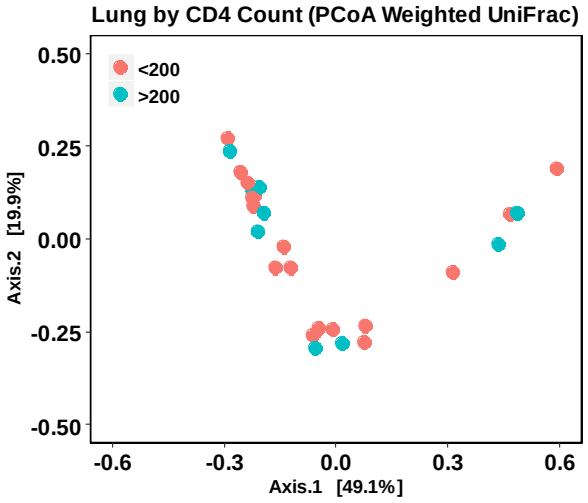

Figure d

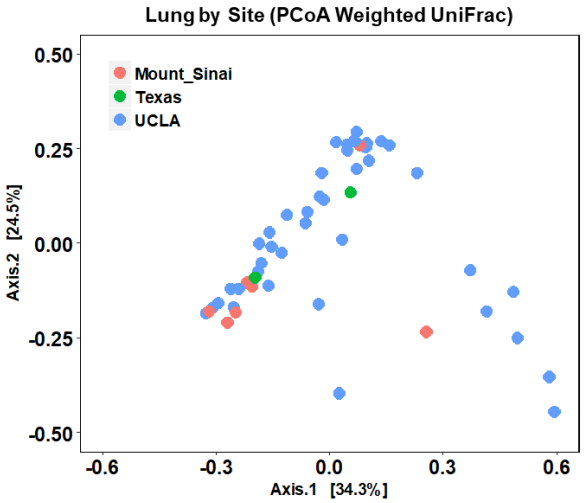

Figure 16. PCoA plot using weighted unifrac of microbial compositions in lungs categorized by telomere length (aTL using kB/SCG 36B4), viral load (copies/mL), CD4 count (cells/mm^3) and clinical site (p-values 0.987, 0.191, 0.903 and 0.228 respectively). Statistical analysis completed using PERMANOVA.

4.3.1.2 Lung Taxonomic Analysis

The figure below shows the relative abundance of major phyla in the lungs of HIV-positive and HIV-negative donors. In both groups Firmicutes and Proteobacteria made up the largest proportion of the microbial community with the rest being mostly Bacteroides, Actinobacteria, Fusobacteria and Verrucomicrobia. Phyla with relative abundance lower than 1% were grouped into the category "Others".

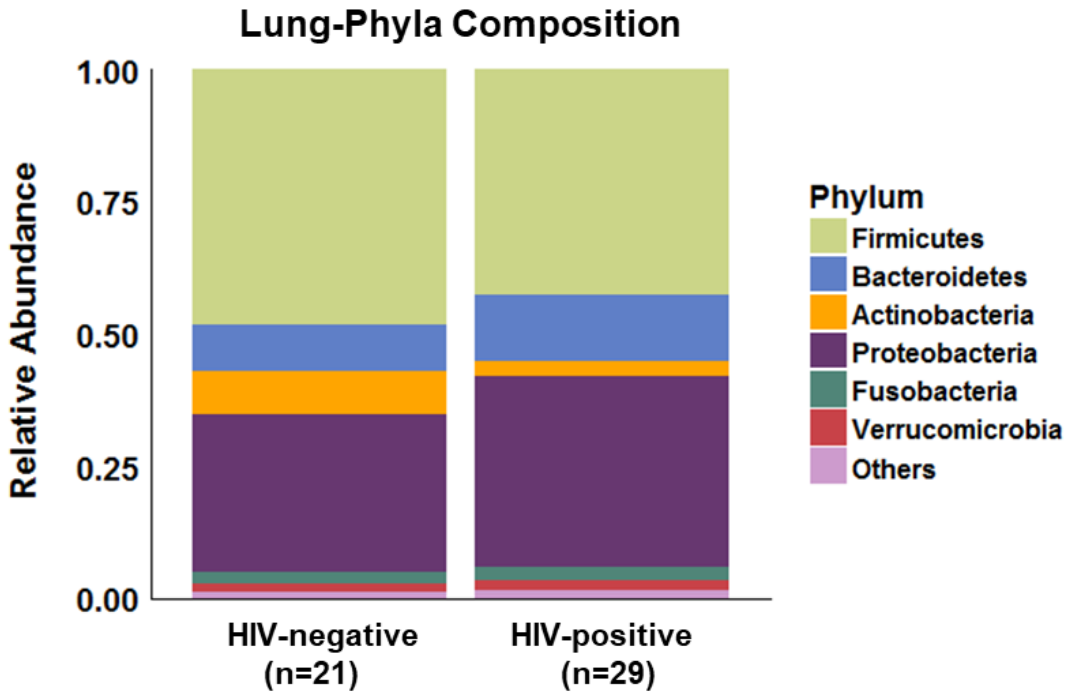

Figure 17. Phyla composition of microbiota in lungs of HIV-positive and HIV-negative donors.

However, statistical analysis using the Wilcoxon rank sum test with continuity correction demonstrated that relative abundance of all major phyla did not differ between HIV-positive and HIV-negative donors in the lung.

Phylum	p-value
Firmicutes	0.504
Bacteroidetes	1.000
Actinobacteria	0.656
Proteobacteria	0.768
Fusobacteria	0.172
Verrucomicrobia	0.428

Table 8. Comparison of major phyla of microbiota in lungs. Comparison between HIV-positive and HIV-negative donors completed using Wilcoxon rank sum test with continuity correction.

Comparison of top 15 genera between HIV-positive and HIV-negative donors demonstrated no significant differences in relative abundance as shown in the table below.

Genus	p-value
Escherichia-Shigella	0.869
Streptococcus	0.533
Lactobacillus	0.834
Staphylococcus	0.475
Veillonella	0.407
Enterococcus	0.599
Paenibacillus	0.357
Prevotella	0.557
Prevotella 7	0.983
Corynebacterium 1	0.524
Proteus	0.332
Bacteroides	0.468
Fusobacterium	0.184
Pseudomonas	0.503
Pelomonas	0.950

Table 9. Comparison of top 15 genera of microbiota in lungs. Comparison between HIV-positive and HIV-negative donors completed using Wilcoxon rank sum test with continuity correction.

Linear discriminant analysis effect size (LEfSe) is a tool used to determine features that would most likely explain differences between groups by combining standard statistical tests with tests for biological consistency and effect relevance. Significant differences were defined as an linear-discriminant analysis (LDA) above 2. In the figure below, in which LDA represents the effect size, four features (Pasteurellales, Pastuerellaceae, Burkholderiaceae and Lactobacillus)

were identified for HIV-positive and three features (Ruminococcus torques, Eisenbergiella and Carnobacteriaceae) for HIV-negative as most likely to explain differences between the two groups.

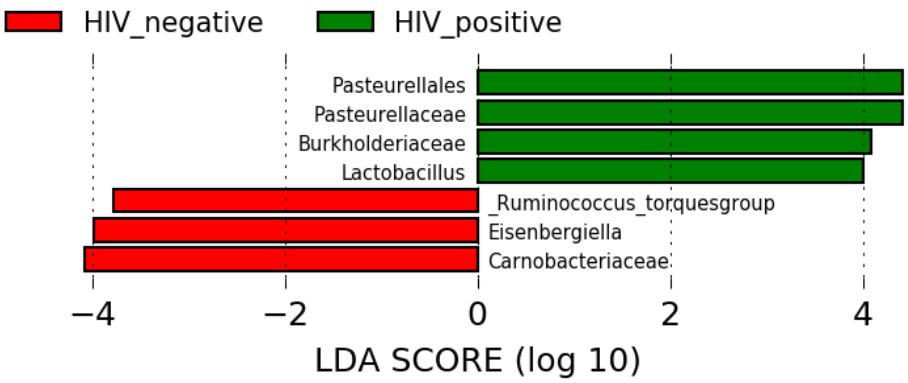

Figure 18. LEfSe analysis on lung microbiota of HIV-positive and HIV-negative donors.

4.3.2 Small Intestine

4.3.2.1 Small Intestine Alpha and Beta Diversity

Alpha diversity measures of observed ASVs (number present), Shannon and Simpson indices were used to quantify diversity within individual small intestine samples. Microbiomes of HIV-positive and HIV-negative donors did not differ in terms of observed ASVs, Shannon index and Simpson index with p-values of 0.242, 0.713 and 0.860 respectively.

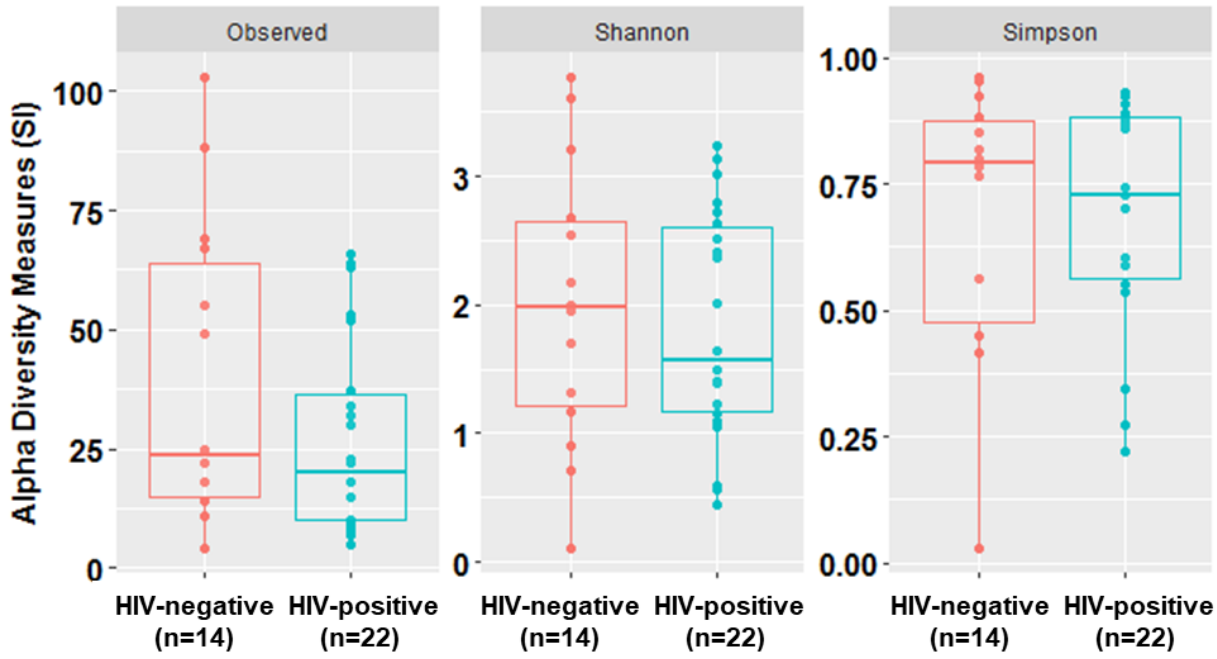

Figure 19. Alpha diversity measures comparing microbiota in small intestine of HIV-positive to HIV-negative donors. Comparisons of observed ASVs, Shannon index and Simpson index yielded p-values of 0.242, 0.713 and 0.860 respectively. Statistical analysis completed using Wilcoxon rank sum test with continuity correction.

Beta diversity analysis was performed for HIV-positive and HIV-negative microbial compositions in the small intestine which were shown to not be statistically different with a p-value of 0.799 using PERMANOVA.

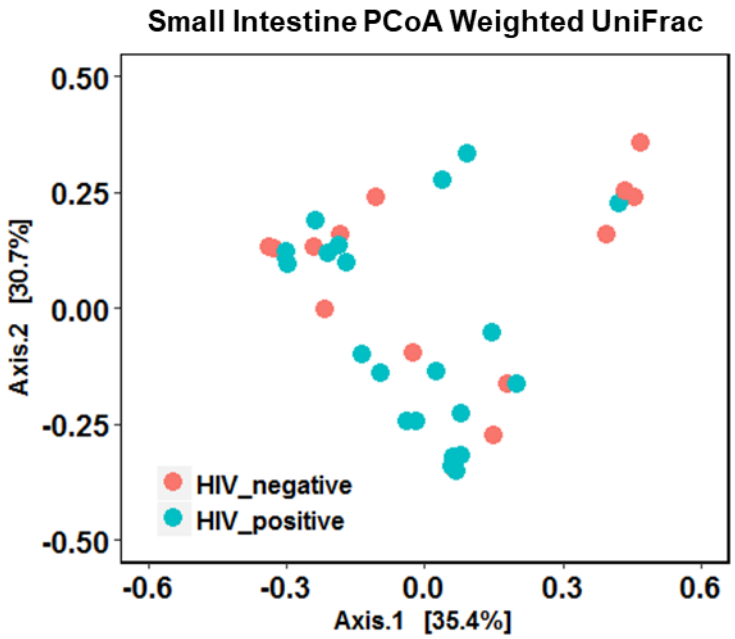

Figure 20. PCoA plot using weighted unifrac of microbial compositions in small intestine of HIV-positive and HIV-negative donors. Statistical analysis completed using PERMANOVA (p=0.799).

Further beta diversity analysis of microbial compositions based on telomere length, viral load, CD4 count and clinical site were performed. Microbial compositions did not differ based as telomere length, viral load and CD4 count with PERMANOVA generated p-values of 0.641, 0.330 and 0.115 respectively. PERMANOVA on clinical site generated a p-value of 0.054, nearing significance.

Figure a

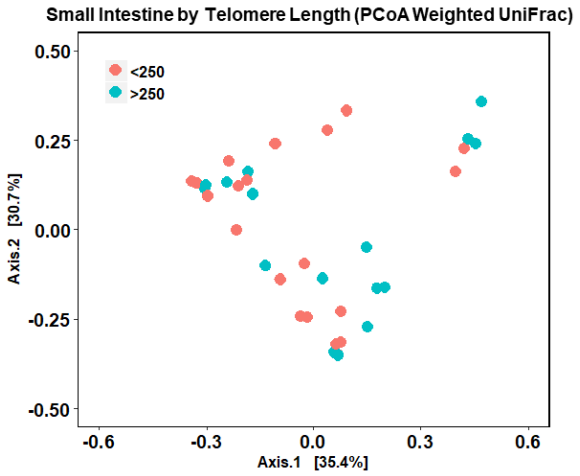

Figure b

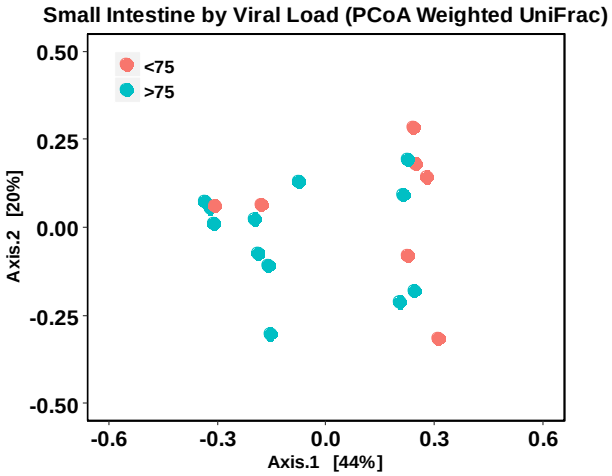

Figure c

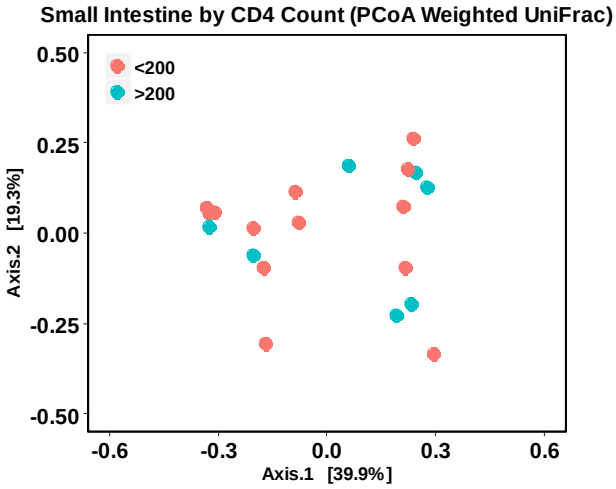

Figure d

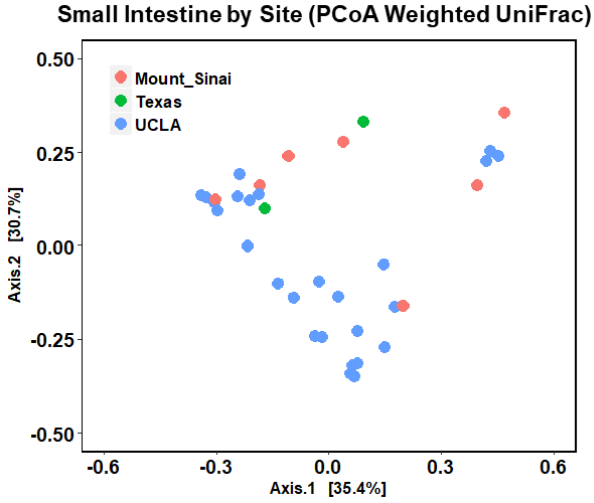

Figure 21. PCoA plot using weighted unifrac of microbial compositions in small intestine categorized by telomere length (aTL using kB/SCG 36B4), viral load (copies/mL), CD4 count (cells/mm^3) and clinical site (p-values 0.641, 0.330, 0.115 and 0.054 respectively). Statistical analysis completed using PERMANOVA.

4.3.2.2 Small Intestine Taxonomic Analysis

The figure below shows the relative abundance of major phyla in small intestine of HIV-positive and HIV-negative donors. Similar to the lung, Firmicutes and Proteobacteria made up the largest proportion of the microbial community with the rest being mostly Bacteroides, Actinobacteria, Fusobacteria and Verrucomicrobia.

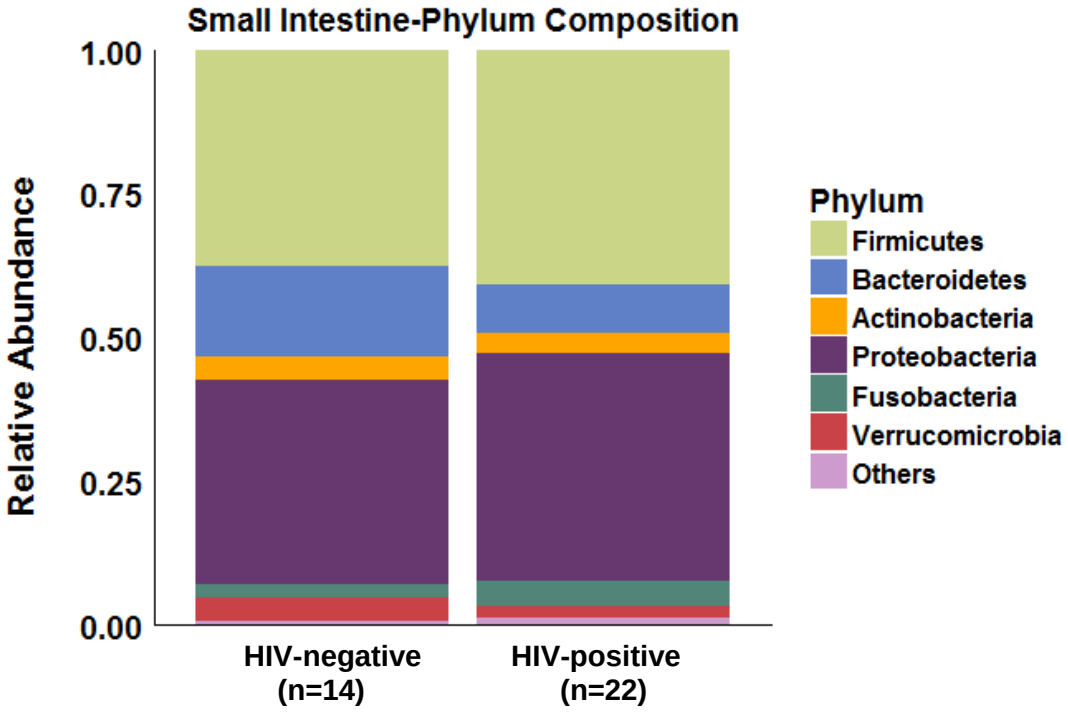

Figure 22. Phyla composition of microbiota in small intestine of HIV-positive and HIV-negative donors.

Statistical analysis using the Wilcoxon rank sum test with continuity correction demonstrated that relative abundance differ significantly only in the Verrucomicrobia phylum when comparing between HIV-positive and HIV-negative donors in small intestine.

Phylum	p-value
Firmicutes	0.884
Bacteroidetes	0.099
Actinobacteria	0.441
Proteobacteria	0.833
Fusobacteria	0.293
Verrucomicrobia	*0.022*

Table 10. Comparison of major phyla of microbiota in small intestine. Comparison between HIV-positive and HIV-negative donors using Wilcoxon rank sum test with continuity correction.

However, the difference in Verrucomicrobia appears to be driven by high relative abundance in a small proportion of samples as shown in the figure below.

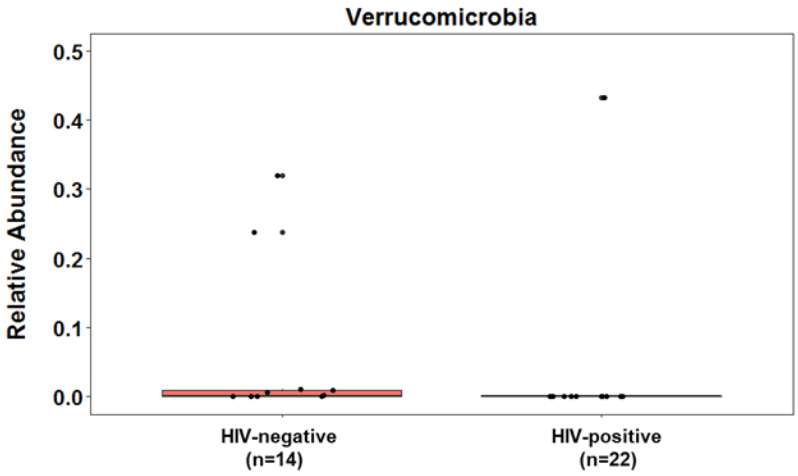

Figure 23. Comparison of relative abundance of Verrucomicrobia between HIV-positive and HIV-negative donors in the small intestine.

Comparison of top 15 genera between HIV-positive and HIV-negative donors demonstrated significant differences in relative abundance of Bacteroides (p=0.021) and Akkermansia (p=0.022) and near significant (p=0.068) in Prevotella.

Genus	p-value
Enterococcus	0.295
Escherichia-Shigella	0.643
Haemophilus	0.591
Bacteroides	*0.021*
Staphylococcus	0.234
Streptococcus	0.401
Lactobacillus	0.756
Fusobacterium	0.276
Proteus	0.345
Akkermansia	*0.022*
Veillonella	0.876
Phyllobacterium	0.964
Parabacteroides	0.182
Faecalibacterium	0.141
Prevotella	*0.068*

Table 11. Comparison of top 15 genera of microbiota in small intestine. Comparison between HIV-positive and HIV-negative donors using Wilcoxon rank sum test with continuity correction.

However, differences in relative abundance of both Akkermansia and Prevotella appeared to be driven by high relative abundance in a few samples as shown in the figures below.

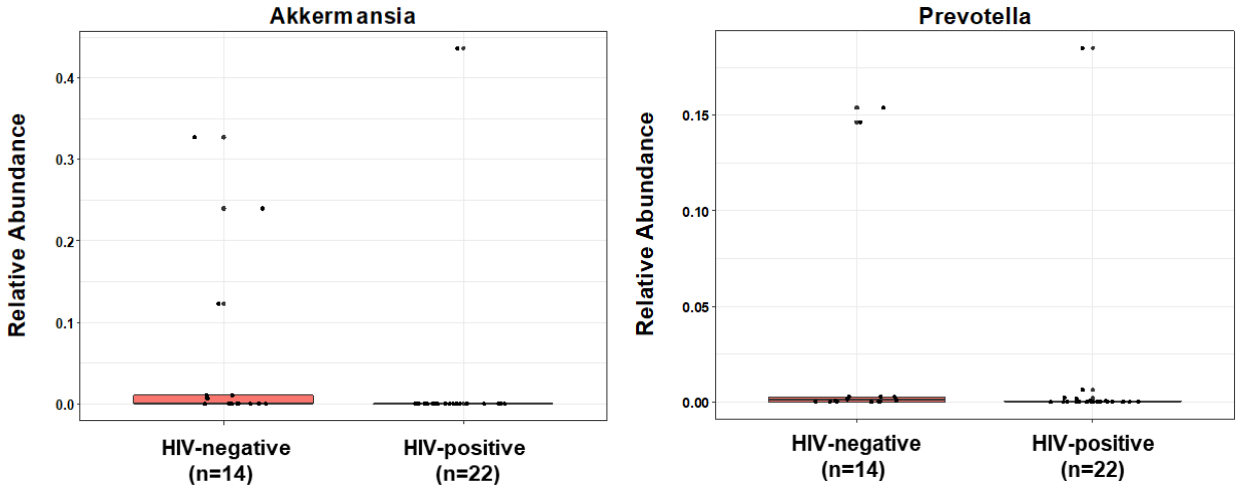

Figure 24. Comparison of relative abundances of Akkermansia and Prevotella between HIV-positive and HIV-negative donors in the small intestine.

Differences in relative abundance of Bacteroides may be a true signal as demonstrated in the figure below.

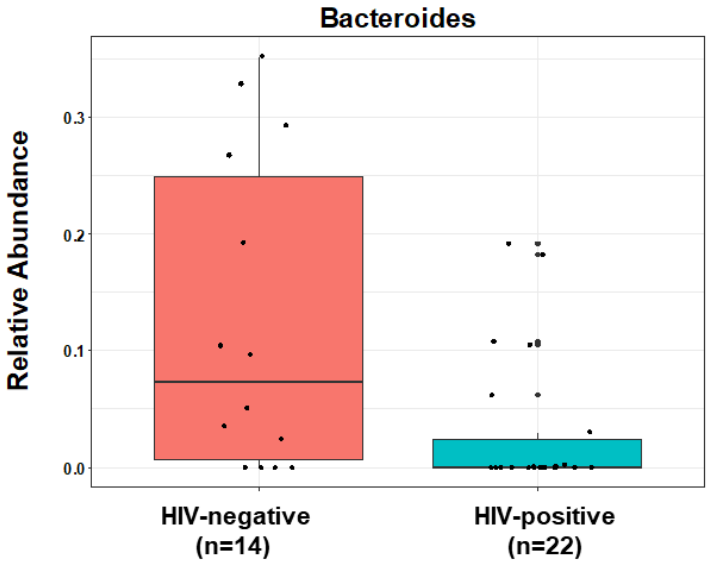

Figure 25. Comparison of relative abundance of Bacteroides between HIV-positive and HIV-negative donors in the small intestine.

LEfSe analysis identified one feature (Ruminococcaceae) for HIV-positive and ten features for HIV-negative that were most likely to explain differences between the two groups.

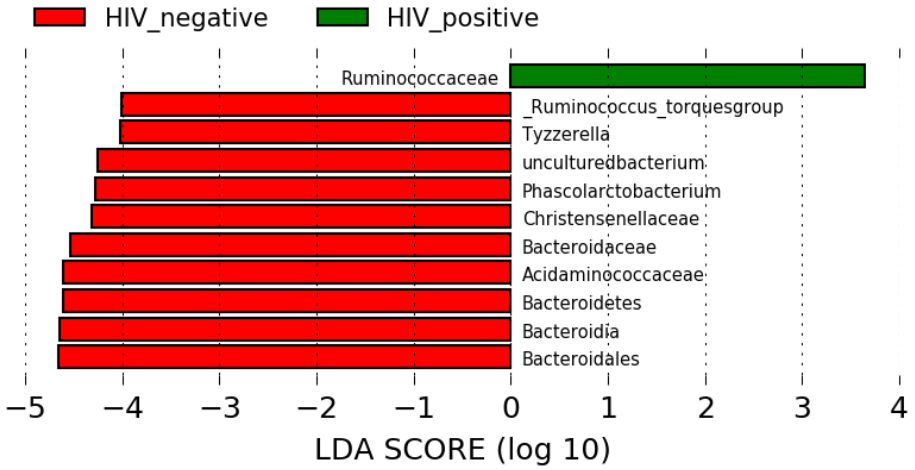

Figure 26. LEfSe analysis on small intestine microbiota of HIV-positive and HIV-negative donors.

4.3.3 Gut-Lung Axis Comparison

Comparison of average ASV abundance in lung and small intestine yielded a significant relationship in both HIV-positive and HIV-negative cohorts ($p<0.0001$ for both). Changes in ASV abundance in the small intestine are related to changes in the same ASV in the lung.

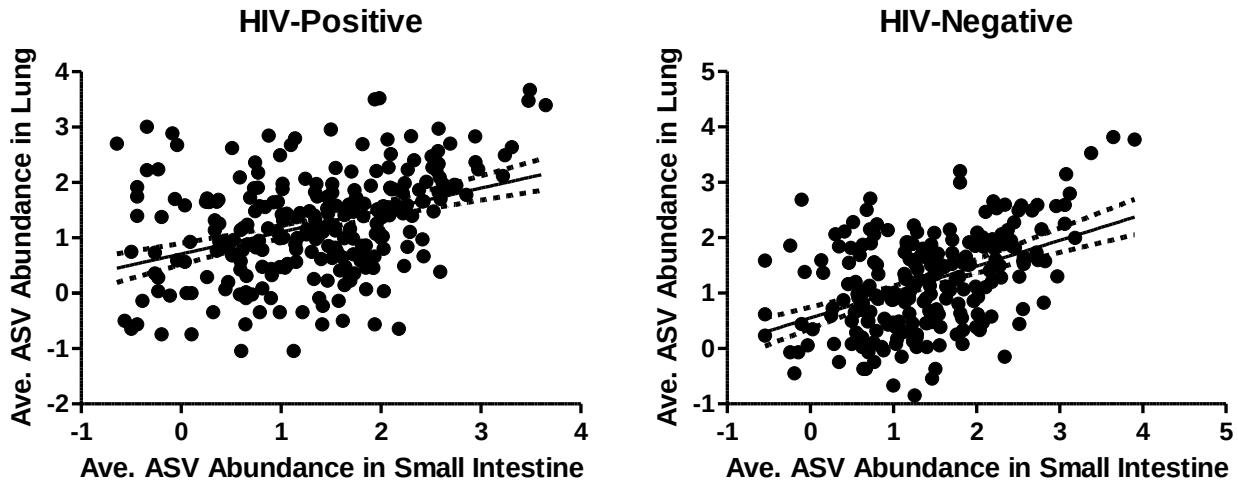

Figure 27. Comparison of average ASV abundance (log transformed) in lungs and small intestine of HIV-positive and HIV-negative donors (both $p<0.0001$). Statistical analysis completed using linear regression. Graph shows best fit line with 95% confidence band.

Chapter 5: Discussion

5.1 Experiment 1: 16S Bacterial Load

In this study, 16S bacterial load was investigated to determine whether bacterial load changes with HIV infection. The results of this cohort demonstrated that HIV infection does not significantly alter bacterial load. Differences in bacterial load between locations (lung and small intestine) were significant as expected. Studies on the lung and gut microbiomes in HIV typically include sequencing data and relative abundances and do not compare bacterial loads between HIV-positive and HIV-negative. However, with multiple studies demonstrating the "normalizing" effect of ART on the microbiome, it is not surprising that the bacterial load does not differ in this cohort of donors who were on ART[89–92].

Evidence of correlation between lung and small intestine 16S bacterial load was shown with a p-value of 0.039 and an R-squared value of 0.126 using linear regression. Although the p-value was below 0.05, the R-squared value was low which indicates that there is some variability of the data from the linear regression model. As samples in this cohort are from autopsies, some donors had pulmonary edema, lung carcinoma and 77% and 73% of HIV-positive and HIV-negative patients had pneumonia respectively. Structural changes as well as bacterial pneumonia may have affected the bacterial load in the lung. As previously mentioned in the introduction, metabolites produced by microbiota of a specific site may affect the immune response in distal sites due to entry into systemic circulation. This could be one factor explaining the correlation between bacterial load in the small intestine and lung in this project.

One of the limitations of this experiment is the inability to dilute lung and small intestine samples to the same dilution which may create bias when comparing the calculated bacterial

load. Small intestine samples without dilution typically exceed the maximum detection limit and therefore a 1:1000 dilution was tested to be the optimal dilution for clear separation. Lung tissue samples are inherently difficult to procure microbial DNA and were diluted to a 1:50 dilution which may cause potential bias when compared to the 1:1000 diluted small intestine samples.

5.2 Experiment 2: Absolute Telomere Length

Comparison of absolute telomere length in the lung and small intestine of HIV-positive and HIV-negative donors demonstrated shortened telomere length in HIV-positive lung in comparison to HIV-negative but no differences in small intestine. This was quite surprising as increased small intestine epithelial turnover has been demonstrated in HIV infection and therefore we hypothesized that aTL would be decreased in HIV-positive donors in comparison to HIV-negative donors. However, sampling location may have an effect on measured aTL as the small intestine samples from this cohort may not all contain tissue from the same cross-section or location. This is one of the limitations in this study as tissue collection was performed by clinical sites in the NNTC consortium and was therefore not controlled specifically for this project. Further comparison of bacterial load and aTL demonstrated no correlation in both lung and small intestine of HIV-positive and HIV-negative donors.

Previous studies have shown aTL to be shorter in peripheral leukocytes and small airway epithelium of HIV-infected individuals[132,134]. In peripheral blood, telomere shortening was observed immediately after HIV seroconversion but not at later time points[135]. Therefore the shortened telomere length demonstrated in the lung of HIV-positive donors may be due to attrition right after HIV infection occurs.

Analysis of the effect of HIV infection on the relationship between aTL and age was not significant in both the lung and small intestine. These results were similar to a study in peripheral lymphocytes where Liu et al demonstrated that slopes of aTL versus age did not differ between HIV-infected and uninfected patients[132]. In the small intestine, these results agree with the previous analysis in which HIV infection did not lead to differences in aTL. In the lung, increased telomere attrition has been shown to occur early on in HIV infection and not in later stages which could be a factor in why the slopes of aTL versus age did not differ when comparing HIV-positive and HIV-negative donors.

5.3 Experiment 3: 16S MiSeq Sequencing

Alpha diversity measures of observed ASVs, Shannon and Simpson indices did not differ when HIV-positive and HIV-negative donors were compared in both lung and small intestine. Analysis of microbial composition using PCoA plot with a weighted UniFrac distance matrix showed no significant difference in microbial composition of HIV-positive and HIV-negative donors in both lung and small intestine. Analysis of beta diversity based on telomere length, viral load, CD4 count and clinical site demonstrated no differences in the lung. The small intestine also demonstrated no differences in beta diversity when samples were categorized based on telomere length, viral load and CD4 count but PERMANOVA analysis on microbial composition categorized by clinical site had a p-value of 0.054. While clinical site may indeed have an effect on microbial composition, uneven sampling depth with only 2 samples from Texas and 27 samples from UCLA may have biased the results in an analysis that compares diversity.

As donors in this cohort were on ART, these results in alpha and beta diversity measures are consistent with existing literature on the HIV lung and gut microbiome[76,131,134]. Microbiomes

of HIV-infected patients on ART are similar to HIV-negative individuals. ART inhibits viral replication and prevents CD4 count decline, helping to avert deterioration of the immune system. Maintenance of the immune response may factor into why the microbiome of ART-treated HIV-infected individuals are comparable to uninfected individuals.

Phyla composition in both lung and small intestine consisted primarily of Firmicutes and Proteobacteria with the remainder comprising mostly of Bacteroides, Actinobacteria, Fusobacteria and Verrucomicrobia. However, comparison of individual phylum in lung and small intestine revealed no significant differences in relative abundance between HIV-positive and HIV-negative donors. Only the Verrucomicrobia phylum in small intestine had a significant difference between HIV-positive and HIV-negative donors with a p-value of 0.022. However, the difference appeared to be driven by high relative abundance in a small proportion of samples. Results on phyla composition in this study are consistent with literature comparing ART-treated HIV patients and uninfected individuals[139,140]. This suggests that ART is effective in maintaining an environment necessary for a "healthy" microbiome.

In the lung, comparison between HIV-positive and HIV-negative relative abundance of the top 15 genera revealed no significant differences in relative abundance. In the small intestine, out of the top 15 genera, the Bacteroides and Akkermansia genera were significantly decreased in relative abundance in HIV-positive donors with p-values of 0.021 and 0.022 respectively. However, the difference in Akkermansia may have been driven by high relative abundance in only a few samples.

In the lung, LEfSe analysis demonstrated four features in HIV-positive (Pasteurellales, Pastuerellaceae, Burkholderiaceae and Lactobacillus) and three features in HIV-negative (Ruminococcus torques, Eisenbergiella and Carnobacteriaceae) that would most likely explain differences between the two experimental groups. One feature (Ruminococcaceae) for HIV-positive and ten features for HIV-negative were identified through LEfSe analysis in the small intestine. In particular, Bacteroidaceae, Bacteroidetes, Bacteroidia and Bacteroidales were found to be significant through LEfSe, corroborating with the previous observation of decreased Bacteroides (genus) in HIV-positive small intestine as the 4 features previously mentioned are all upstream taxonomic classifications of Bacteroides. Previous studies have also found decreased Bacteroides in HIV-positive subjects in comparison to HIV-negative subjects[69]. This suggests that changes due to HIV infection, potentially in immune function, lead to decreased Bacteroides although no mechanism has been described thus far. Although other features have been discovered through LEfSe to potentially explain difference between the two experimental groups, identification of the same features in separate studies would be required as many other studies have also identified potential bacterial markers but have not been able to replicate the results.

Average abundance of individual ASV was demonstrated to be correlated in the lung and small intestine in both HIV-positive and HIV-negative groups ($p<0.0001$ for both). One potential explanation may be the overlap of factors that influence microbial composition such as environment, host immune system and oral sources. Whether and how communication between the two physically separate microbiomes could result in a relationship between abundance of the same bacteria in the two sites has yet to be studied.

Chapter 6: Conclusion

This project identified correlations in microbiotas of the gut-lung axis in terms of bacterial load and abundance of individual ASVs. ART-treated HIV donors did not demonstrate a significant difference in microbial composition in comparison to HIV-negative donors and categorization by host characteristics such as telomere length, CD4 count and viral load also did not reveal differences in microbial composition between the two experimental groups in both the lung and small intestine. Shortened telomere length was shown in the HIV-positive lung in comparison to the HIV-negative group but no differences were seen in small intestine.

In terms of phyla composition, HIV-positive and HIV-negative groups did not demonstrate significant differences in phyla relative abundance in both lung and small intestine. Genus Bacteroides in the small intestine was found to be decreased in HIV-positive donors. Furthermore, LEfSe identified the family Bacteroidaceae (under phylum Bacteroidetes, class Bacteroidia and order Bacteroidales, all of which were identified in LEfSe) in the small intestine to be one of the features most likely to explain the differences between the HIV-positive and HIV-negative groups. These results corroborated with previous analysis of the genus Bacteroides being decreased in HIV-positive small intestine.

This study was limited in its cross-sectional nature, sampling only post-mortem samples. An improved study design would include serial samples from patients starting at a time point prior to HIV seroconversion. Tissue sampling was also a limitation in this study as tissues sampled may not have been from the same cross-section or anatomical location in the lung and small intestine. Procedural controls for tissue sampling detailing sample site and cross-sectional area would help overcome these limitations. However, random sampling location could result in

non-systematic bias, leading to overestimated p-values in this study. Changes in microbiome could occur due to post-mortem changes prior to storage in -80°C and differences in length of HIV-infection, ART regimen and concomitant medications.

Future studies with controlled sample collection, targeted sampling technique and increased sample size would be able to overcome some of the limitations in this project. Interventional studies in the microbiome are required to further the field in investigating the exact mechanisms in which the gut-lung axis communicate and affect each other. Furthermore, development of new statistical tools may be required for analysis of results exploring relationships between two separate ecosystems. Overall, the results from this thesis show that ART-treated HIV patients present microbiota similar to HIV-negative patients, demonstrating the ability of ART to provide the microenvironment necessary to maintain a "healthy" microbiome. Decreased Bacteroides in the small intestine may be a potential identifier of HIV infection and could be a result of immune dysfunction processes specific to HIV. Furthermore, microbiomes of the gut-lung axis have demonstrated a correlation in bacterial load and abundance of individuals ASVs, with the latter suggesting a strong relationship between abundances of overlap bacteria between the two sites.

Bibliography

1. Fact sheet - Latest statistics on the status of the AIDS epidemic | UNAIDS. Available at: http://www.unaids.org/en/resources/fact-sheet. (Accessed: 20th July 2018)
2. WHO | HIV/AIDS. *WHO* (2018). Available at: http://www.who.int/hiv/en/ (Accessed: 20th July 2018)
3. Bourgeois, A. C. *et al.* HIV in Canada-Surveillance Report, 2016. **43,** 12
4. German Advisory Committee Blood (Arbeitskreis Blut), Subgroup 'Assessment of Pathogens Transmissible by Blood', G. A. C. B. (Arbeitskreis & Blood', S. 'Assessment of P. T. by. Human Immunodeficiency Virus (HIV). *Transfus. Med. Hemother.* **43,** 203–22 (2016).
5. Fettig, J., Swaminathan, M., Murrill, C. S. & Kaplan, J. E. Global Epidemiology of HIV. *Infect. Dis. Clin. North Am.* **28,** 323–337 (2014).
6. *UPDATE ON HIV-1 STRAIN AND TRANSMITTED DRUG RESISTANCE IN CANADA*. (2017). Available at: http://publications.gc.ca/site/eng/9.843746/publication.html. (Accessed: 20th July 2018)
7. *A TIMELINE OF HIV/AIDS*. Available at: https://www.hiv.gov/sites/default/files/aidsgov-timeline.pdf. (Accessed: 20th July 2018)
8. *A history of HIV/AIDS*. Available at: http://www.catie.ca/en/printpdf/world-aids-day/history. (Accessed: 20th July 2018)
9. Bhatti, A. B., Usman, M. & Kandi, V. Current Scenario of HIV/AIDS, Treatment Options, and Major Challenges with Compliance to Antiretroviral Therapy. *Cureus* **8,** e515 (2016).
10. Simon, V., Ho, D. D. & Abdool Karim, Q. HIV/AIDS epidemiology, pathogenesis, prevention, and treatment. *Lancet (London, England)* **368,** 489–504 (2006).

11. Jones, A. *et al.* Transformation of HIV from pandemic to low-endemic levels: a public health approach to combination prevention. *Lancet* **384,** 272–279 (2014).

12. Samji, H. *et al.* Closing the gap: increases in life expectancy among treated HIV-positive individuals in the United States and Canada. *PLoS One* **8,** e81355 (2013).

13. World Health Organization & World Health Organization. Department of HIV/AIDS. *Guideline on when to start antiretroviral therapy and on pre-exposure prophylaxis for HIV.*

14. Group, T. I. S. S. Initiation of Antiretroviral Therapy in Early Asymptomatic HIV Infection. *N. Engl. J. Med.* **373,** 795–807 (2015).

15. Maartens, G., Celum, C. & Lewin, S. R. HIV infection: epidemiology, pathogenesis, treatment, and prevention. *Lancet* **384,** 258–271 (2014).

16. Nazli, A. *et al.* Exposure to HIV-1 directly impairs mucosal epithelial barrier integrity allowing microbial translocation. *PLoS Pathog.* **6,** e1000852 (2010).

17. Deeks, S. G., Lewin, S. R. & Havlir, D. V. The end of AIDS: HIV infection as a chronic disease. *Lancet* **382,** 1525–1533 (2013).

18. Sender, R., Fuchs, S. & Milo, R. Revised Estimates for the Number of Human and Bacteria Cells in the Body. *PLOS Biol.* **14,** e1002533 (2016).

19. Ursell, L. K., Metcalf, J. L., Parfrey, L. W. & Knight, R. Defining the human microbiome. *Nutr. Rev.* **70 Suppl 1,** S38-44 (2012).

20. Cole, J. R. *et al.* Ribosomal Database Project: data and tools for high throughput rRNA analysis. *Nucleic Acids Res.* **42,** D633–D642 (2014).

21. Balvočiūtė, M. & Huson, D. H. SILVA, RDP, Greengenes, NCBI and OTT — how do these taxonomies compare? *BMC Genomics* **18,** 114 (2017).

22. DeSantis, T. Z. *et al.* Greengenes, a Chimera-Checked 16S rRNA Gene Database and Workbench Compatible with ARB. *Appl. Environ. Microbiol.* **72,** 5069–5072 (2006).

23. Pruesse, E. *et al.* SILVA: a comprehensive online resource for quality checked and aligned ribosomal RNA sequence data compatible with ARB. *Nucleic Acids Res.* **35,** 7188–7196 (2007).

24. Dominguez-Bello, M. G. *et al.* Delivery mode shapes the acquisition and structure of the initial microbiota across multiple body habitats in newborns. *Proc. Natl. Acad. Sci. U. S. A.* **107,** 11971–5 (2010).

25. Koenig, J. E. *et al.* Succession of microbial consortia in the developing infant gut microbiome. *Proc. Natl. Acad. Sci. U. S. A.* **108 Suppl 1,** 4578–85 (2011).

26. Fierer, N. *et al.* Forensic identification using skin bacterial communities. *Proc. Natl. Acad. Sci. U. S. A.* **107,** 6477–81 (2010).

27. Heederik, D. & von Mutius, E. Does diversity of environmental microbial exposure matter for the occurrence of allergy and asthma? *J. Allergy Clin. Immunol.* **130,** 44–50 (2012).

28. Ege, M. J. *et al.* Exposure to Environmental Microorganisms and Childhood Asthma. *N. Engl. J. Med.* **364,** 701–709 (2011).

29. Riedler, J. *et al.* Exposure to farming in early life and development of asthma and allergy: a cross-sectional survey. *Lancet* **358,** 1129–1133 (2001).

30. Ownby, D. R., Johnson, C. C. & Peterson, E. L. Exposure to Dogs and Cats in the First Year of Life and Risk of Allergic Sensitization at 6 to 7 Years of Age. *JAMA* **288,** 963 (2002).

31. Waser, M. *et al.* Inverse association of farm milk consumption with asthma and allergy in rural and suburban populations across Europe. *Clin. Exp. Allergy* **37,** 661–670 (2007).

32. Peterson, J. *et al.* The NIH Human Microbiome Project. *Genome Res.* **19,** 2317–2323 (2009).

33. Gevers, D. *et al.* The Human Microbiome Project: A Community Resource for the Healthy Human Microbiome. *PLoS Biol.* **10,** e1001377 (2012).

34. Turnbaugh, P. J. *et al.* The human microbiome project. *Nature* **449,** 804–10 (2007).

35. Integrative HMP (iHMP) Research Network Consortium. The Integrative Human Microbiome Project: Dynamic Analysis of Microbiome-Host Omics Profiles during Periods of Human Health and Disease. *Cell Host Microbe* **16,** 276–289 (2014).

36. Rodríguez, J. M. *et al.* The composition of the gut microbiota throughout life, with an emphasis on early life. *Microb. Ecol. Health Dis.* **26,** 26050 (2015).

37. Koenig, J. E. *et al.* Succession of microbial consortia in the developing infant gut microbiome. *Proc. Natl. Acad. Sci. U. S. A.* **108 Suppl 1,** 4578–85 (2011).

38. Claesson, M. J. *et al.* Composition, variability, and temporal stability of the intestinal microbiota of the elderly. *Proc. Natl. Acad. Sci. U. S. A.* **108 Suppl 1,** 4586–91 (2011).

39. Biagi, E. *et al.* Through Ageing, and Beyond: Gut Microbiota and Inflammatory Status in Seniors and Centenarians. *PLoS One* **5,** e10667 (2010).

40. Woodmansey, E. J., McMurdo, M. E. T., Macfarlane, G. T. & Macfarlane, S. Comparison of compositions and metabolic activities of fecal microbiotas in young adults and in antibiotic-treated and non-antibiotic-treated elderly subjects. *Appl. Environ. Microbiol.* **70,** 6113–22 (2004).

41. Lozupone, C. A., Stombaugh, J. I., Gordon, J. I., Jansson, J. K. & Knight, R. Diversity, stability and resilience of the human gut microbiota. *Nature* **489,** 220–30 (2012).

42. Bäckhed, F. Programming of Host Metabolism by the Gut Microbiota. *Ann. Nutr. Metab.*

58, 44–52 (2011).

43. David, L. A. *et al.* Diet rapidly and reproducibly alters the human gut microbiome. *Nature* **505,** 559–563 (2014).

44. Jiang, H. *et al.* Altered fecal microbiota composition in patients with major depressive disorder. *Brain. Behav. Immun.* **48,** 186–194 (2015).

45. Biedermann, L. *et al.* Smoking Cessation Induces Profound Changes in the Composition of the Intestinal Microbiota in Humans. *PLoS One* **8,** e59260 (2013).

46. Tyakht, A. V. *et al.* Human gut microbiota community structures in urban and rural populations in Russia. *Nat. Commun.* **4,** 2469 (2013).

47. Jernberg, C., Löfmark, S., Edlund, C. & Jansson, J. K. Long-term ecological impacts of antibiotic administration on the human intestinal microbiota. *ISME J.* **1,** 56–66 (2007).

48. Ley, R. E., Peterson, D. A. & Gordon, J. I. Ecological and Evolutionary Forces Shaping Microbial Diversity in the Human Intestine. *Cell* **124,** 837–848 (2006).

49. Macpherson, A. J. & McCoy, K. D. Stratification and compartmentalisation of immunoglobulin responses to commensal intestinal microbes. *Semin. Immunol.* **25,** 358–363 (2013).

50. Rogier, E. *et al.* Secretory IgA is Concentrated in the Outer Layer of Colonic Mucus along with Gut Bacteria. *Pathogens* **3,** 390–403 (2014).

51. Wehkamp, J. *et al.* Reduced Paneth cell alpha-defensins in ileal Crohn's disease. *Proc. Natl. Acad. Sci. U. S. A.* **102,** 18129–34 (2005).

52. Donaldson, G. P., Lee, S. M. & Mazmanian, S. K. Gut biogeography of the bacterial microbiota. *Nat. Rev. Microbiol.* **14,** 20–32 (2016).

53. Thursby, E. & Juge, N. Introduction to the human gut microbiota. *Biochem. J.* **474,** 1823–

1836 (2017).

54. Pompei, A. *et al.* Folate production by bifidobacteria as a potential probiotic property. *Appl. Environ. Microbiol.* **73,** 179–85 (2007).

55. Hill, M. J. Intestinal flora and endogenous vitamin synthesis. *Eur. J. Cancer Prev.* **6 Suppl 1,** S43-5 (1997).

56. Martens, H. Barg, M. Warren, D. Jah, J.-H., Barg, H., Warren, M. J. & Jahn, D. Microbial production of vitamin B 12. *Appl. Microbiol. Biotechnol.* **58,** 275–285 (2002).

57. LeBlanc, J. G. *et al.* Bacteria as vitamin suppliers to their host: a gut microbiota perspective. *Curr. Opin. Biotechnol.* **24,** 160–168 (2013).

58. Chen, H.-Q. *et al.* Lactobacillus plantarum ameliorates colonic epithelial barrier dysfunction by modulating the apical junctional complex and PepT1 in IL-10 knockout mice. *Am. J. Physiol. Liver Physiol.* **299,** G1287–G1297 (2010).

59. Swanson, P. A. *et al.* Enteric commensal bacteria potentiate epithelial restitution via reactive oxygen species-mediated inactivation of focal adhesion kinase phosphatases. *Proc. Natl. Acad. Sci. U. S. A.* **108,** 8803–8 (2011).

60. Reunanen, J. *et al.* Akkermansia muciniphila Adheres to Enterocytes and Strengthens the Integrity of the Epithelial Cell Layer. *Appl. Environ. Microbiol.* **81,** 3655–62 (2015).

61. Bäumler, A. J. & Sperandio, V. Interactions between the microbiota and pathogenic bacteria in the gut. *Nature* **535,** 85–93 (2016).

62. Morrison, D. J. & Preston, T. Formation of short chain fatty acids by the gut microbiota and their impact on human metabolism. *Gut Microbes* **7,** 189–200 (2016).

63. Smith, K., McCoy, K. D. & Macpherson, A. J. Use of axenic animals in studying the adaptation of mammals to their commensal intestinal microbiota. *Semin. Immunol.* **19,** 59–

69 (2007).

64. Dubourg, G. Impact of HIV on the human gut microbiota: Challenges and perspectives. *Hum. Microbiome J.* **2,** 3–9 (2016).

65. McHardy, I. H. *et al.* HIV Infection is associated with compositional and functional shifts in the rectal mucosal microbiota. *Microbiome* **1,** 26 (2013).

66. Ling, Z. *et al.* Alterations in the Fecal Microbiota of Patients with HIV-1 Infection: An Observational Study in A Chinese Population. *Sci. Rep.* **6,** 30673 (2016).

67. Dillon, S. M. *et al.* An altered intestinal mucosal microbiome in HIV-1 infection is associated with mucosal and systemic immune activation and endotoxemia. *Mucosal Immunol.* **7,** 983–994 (2014).

68. Mutlu, E. A. *et al.* A Compositional Look at the Human Gastrointestinal Microbiome and Immune Activation Parameters in HIV Infected Subjects. *PLoS Pathog.* **10,** e1003829 (2014).

69. Lozupone, C. A. *et al.* HIV-induced alteration in gut microbiota. *Gut Microbes* **5,** 562–570 (2014).

70. Dillon, S. M. *et al.* An altered intestinal mucosal microbiome in HIV-1 infection is associated with mucosal and systemic immune activation and endotoxemia. *Mucosal Immunol.* **7,** 983–994 (2014).

71. Mutlu, E. A. *et al.* A Compositional Look at the Human Gastrointestinal Microbiome and Immune Activation Parameters in HIV Infected Subjects. *PLoS Pathog.* **10,** e1003829 (2014).

72. Lozupone, C. A. *et al.* Alterations in the Gut Microbiota Associated with HIV-1 Infection. *Cell Host Microbe* **14,** 329–339 (2013).

73. Monaco, C. L. *et al.* Altered Virome and Bacterial Microbiome in Human Immunodeficiency Virus-Associated Acquired Immunodeficiency Syndrome. (2016). doi:10.1016/j.chom.2016.02.011

74. Nowak, P. *et al.* Gut microbiota diversity predicts immune status in HIV-1 infection. *AIDS* **29,** 2409–2418 (2015).

75. Noguera-Julian, M. *et al.* Gut Microbiota Linked to Sexual Preference and HIV Infection. *EBioMedicine* **5,** 135–146 (2016).

76. Dinh, D. M. *et al.* Intestinal Microbiota, Microbial Translocation, and Systemic Inflammation in Chronic HIV Infection. *J. Infect. Dis.* **211,** 19–27 (2015).

77. Burgener, A., McGowan, I. & Klatt, N. R. HIV and mucosal barrier interactions: consequences for transmission and pathogenesis. *Curr. Opin. Immunol.* **36,** 22–30 (2015).

78. Dickson, R. P., Erb-Downward, J. R., Martinez, F. J. & Huffnagle, G. B. The Microbiome and the Respiratory Tract. *Annu. Rev. Physiol.* **78,** 481–504 (2016).

79. Wilson, M. T. & Hamilos, D. L. The Nasal and Sinus Microbiome in Health and Disease. *Curr. Allergy Asthma Rep.* **14,** 485 (2014).

80. Erb-Downward, J. R. *et al.* Analysis of the Lung Microbiome in the "Healthy" Smoker and in COPD. *PLoS One* **6,** e16384 (2011).

81. Charlson, E. S. *et al.* Lung-enriched Organisms and Aberrant Bacterial and Fungal Respiratory Microbiota after Lung Transplant. *Am. J. Respir. Crit. Care Med.* **186,** 536–545 (2012).

82. Yatsunenko, T. *et al.* Human gut microbiome viewed across age and geography. *Nature* **486,** 222–227 (2012).

83. Biesbroek, G. *et al.* Early Respiratory Microbiota Composition Determines Bacterial

Succession Patterns and Respiratory Health in Children. *Am. J. Respir. Crit. Care Med.* **190,** 1283–1292 (2014).

84. Burke, D. G. *et al.* The altered gut microbiota in adults with cystic fibrosis. *BMC Microbiol.* **17,** 58 (2017).

85. Huang, Y. J. & LiPuma, J. J. The Microbiome in Cystic Fibrosis. *Clin. Chest Med.* **37,** 59–67 (2016).

86. Sze, M. A. *et al.* The lung tissue microbiome in chronic obstructive pulmonary disease. *Am. J. Respir. Crit. Care Med.* **185,** 1073–80 (2012).

87. Huang, Y. J. & Boushey, H. A. The microbiome in asthma. *J. Allergy Clin. Immunol.* **135,** 25–30 (2015).

88. Hilty, M. *et al.* Disordered Microbial Communities in Asthmatic Airways. *PLoS One* **5,** e8578 (2010).

89. Twigg, H. L. *et al.* Effect of advanced HIV infection on the respiratory microbiome. *Am. J. Respir. Crit. Care Med.* (2016). doi:10.1164/rccm.201509-1875OC

90. Cui, L. *et al.* Topographic diversity of the respiratory tract mycobiome and alteration in HIV and lung disease. *Am. J. Respir. Crit. Care Med.* (2015). doi:10.1164/rccm.201409-1583OC

91. Beck, J. M. *et al.* Multicenter comparison of lung and oral microbiomes of HIV-infected and HIV-uninfected individuals. *Am. J. Respir. Crit. Care Med.* (2015). doi:10.1164/rccm.201501-0128OC

92. Lozupone, C. *et al.* Widespread colonization of the lung by Tropheryma whipplei in HIV infection. *Am. J. Respir. Crit. Care Med.* (2013). doi:10.1164/rccm.201211-2145OC

93. Larsen, J. M. The immune response to Prevotella bacteria in chronic inflammatory

disease. *Immunology* **151,** 363–374 (2017).

94. MORRIS, A. M. *et al.* Permanent Declines in Pulmonary Function Following Pneumonia in Human Immunodeficiency Virus-Infected Persons. *Am. J. Respir. Crit. Care Med.* **162,** 612–616 (2000).

95. Sogaard, O. S. *et al.* Hospitalization for Pneumonia among Individuals With and Without HIV Infection, 1995–2007: A Danish Population-Based, Nationwide Cohort Study. *Clin. Infect. Dis.* **47,** 1345–1353 (2008).

96. Bénard, A. *et al.* Bacterial pneumonia among HIV-infected patients: decreased risk after tobacco smoking cessation. ANRS CO3 Aquitaine Cohort, 2000-2007. *PLoS One* **5,** e8896 (2010).

97. Segal, L. N. *et al.* HIV-1 and bacterial pneumonia in the era of antiretroviral therapy. *Proc. Am. Thorac. Soc.* **8,** 282–7 (2011).

98. Iwai, S. *et al.* Oral and airway microbiota in HIV-infected pneumonia patients. *J. Clin. Microbiol.* **50,** 2995–3002 (2012).

99. Roussos, A., Koursarakos, P., Patsopoulos, D., Gerogianni, I. & Philippou, N. Increased prevalence of irritable bowel syndrome in patients with bronchial asthma. *Respir. Med.* **97,** 75–9 (2003).

100. Rutten, E. P. A., Lenaerts, K., Buurman, W. A. & Wouters, E. F. M. Disturbed Intestinal Integrity in Patients With COPD. *Chest* **145,** 245–252 (2014).

101. Budden, K. F. *et al.* Emerging pathogenic links between the microbiota and the gut–lung axis. (2016). doi:10.1038/nrmicro.2016.142

102. Al-Asmakh, M. & Zadjali, F. Use of Germ-Free Animal Models in Microbiota-Related Research. *J. Microbiol. Biotechnol.* **25,** 1583–1588 (2015).

103. Wymore Brand, M. *et al.* The Altered Schaedler Flora: Continued Applications of a Defined Murine Microbial Community. *ILAR J.* **56,** 169–178 (2015).

104. Dickson, R. P. *et al.* Enrichment of the lung microbiome with gut bacteria in sepsis and the acute respiratory distress syndrome. *Nat. Microbiol.* **1,** 16113 (2016).

105. Reibman, J. *et al.* Asthma Is Inversely Associated with Helicobacter pylori Status in an Urban Population. *PLoS One* **3,** e4060 (2008).

106. Chen, Y. & Blaser, M. J. Inverse Associations of Helicobacter pylori With Asthma and Allergy. *Arch. Intern. Med.* **167,** 821 (2007).

107. Chen, Y. & Blaser, M. J. *Helicobacter pylori* Colonization Is Inversely Associated with Childhood Asthma. *J. Infect. Dis.* **198,** 553–560 (2008).

108. Wang, F., Liu, J., Zhang, Y. & Lei, P. Association of *Helicobacter pylori* infection with chronic obstructive pulmonary disease and chronic bronchitis: a meta-analysis of 16 studies. *Infect. Dis. (Auckl).* **47,** 597–603 (2015).

109. Trompette, A. *et al.* Gut microbiota metabolism of dietary fiber influences allergic airway disease and hematopoiesis. *Nat. Med.* **20,** 159–166 (2014).

110. Gauguet, S. *et al.* Intestinal Microbiota of Mice Influences Resistance to Staphylococcus aureus Pneumonia. *Infect. Immun.* **83,** 4003–4014 (2015).

111. Vieira, A. T. *et al.* Control of Klebsiella pneumoniae pulmonary infection and immunomodulation by oral treatment with the commensal probiotic Bifidobacterium longum 5 1A. *Microbes Infect.* **18,** 180–189 (2016).

112. Kawahara, T. *et al.* Consecutive oral administration of *Bifidobacterium longum* MM-2 improves the defense system against influenza virus infection by enhancing natural killer cell activity in a murine model. *Microbiol. Immunol.* **59,** 1–12 (2015).

113. Sze, M. A. *et al.* Changes in the Bacterial Microbiota in Gut, Blood, and Lungs following Acute LPS Instillation into Mice Lungs. *PLoS One* **9,** e111228 (2014).

114. Heaton, R. K. *et al.* HIV-associated neurocognitive disorders persist in the era of potent antiretroviral therapy: CHARTER Study. *Neurology* **75,** 2087–2096 (2010).

115. Rasmussen, L. D. *et al.* Time trends for risk of severe age-related diseases in individuals with and without HIV infection in Denmark: a nationwide population-based cohort study. *Lancet HIV* **2,** e288–e298 (2015).

116. Kooij, K. W. *et al.* Low Bone Mineral Density in Patients With Well-Suppressed HIV Infection: Association With Body Weight, Smoking, and Prior Advanced HIV Disease. *J. Infect. Dis.* **211,** 539–548 (2015).

117. Thiara, D. K. *et al.* Abnormal Myocardial Function Is Related to Myocardial Steatosis and Diffuse Myocardial Fibrosis in HIV-Infected Adults. *J. Infect. Dis.* **212,** 1544–1551 (2015).

118. Angelovich, T. A. *et al.* Viremic and Virologically Suppressed HIV Infection Increases Age-Related Changes to Monocyte Activation Equivalent to 12 and 4 Years of Aging, Respectively. *JAIDS J. Acquir. Immune Defic. Syndr.* **69,** 11–17 (2015).

119. Naeger, D. M. *et al.* Cytomegalovirus-Specific T Cells Persist at Very High Levels during Long-Term Antiretroviral Treatment of HIV Disease. *PLoS One* **5,** e8886 (2010).

120. Lorenzo-Redondo, R. *et al.* Persistent HIV-1 replication maintains the tissue reservoir during therapy. *Nature* **530,** 51–56 (2016).

121. Franceschi, C. *et al.* Inflamm-aging. An evolutionary perspective on immunosenescence. *Ann. N. Y. Acad. Sci.* **908,** 244–54 (2000).

122. May, M. T. *et al.* Impact on life expectancy of HIV-1 positive individuals of CD4+ cell

count and viral load response to antiretroviral therapy. *AIDS* **28,** 1193–1202 (2014).

123. May, M. *et al.* Impact of late diagnosis and treatment on life expectancy in people with HIV-1: UK Collaborative HIV Cohort (UK CHIC) Study. *BMJ* **343,** d6016 (2011).

124. Althoff, K. N. *et al.* Comparison of Risk and Age at Diagnosis of Myocardial Infarction, End-Stage Renal Disease, and Non-AIDS-Defining Cancer in HIV-Infected Versus Uninfected Adults. *Clin. Infect. Dis.* **60,** 627–638 (2015).

125. Freiberg, M. S. *et al.* HIV Infection and the Risk of Acute Myocardial Infarction. *JAMA Intern. Med.* **173,** 614 (2013).

126. Sico, J. J. *et al.* HIV status and the risk of ischemic stroke among men. *Neurology* **84,** 1933–1940 (2015).

127. Prieto-Alhambra, D. *et al.* HIV Infection and Its Association With an Excess Risk of Clinical Fractures. *JAIDS J. Acquir. Immune Defic. Syndr.* **66,** 90–95 (2014).

128. López-Otín, C., Blasco, M. A., Partridge, L., Serrano, M. & Kroemer, G. The Hallmarks of Aging. *Cell* **153,** 1194–1217 (2013).

129. Sanders, J. L. & Newman, A. B. Telomere length in epidemiology: a biomarker of aging, age-related disease, both, or neither? *Epidemiol. Rev.* **35,** 112–31 (2013).

130. Prasad, K. N., Wu, M. & Bondy, S. C. Telomere shortening during aging: Attenuation by antioxidants and anti-inflammatory agents. *Mech. Ageing Dev.* **164,** 61–66 (2017).

131. Starkweather, A. R. *et al.* An integrative review of factors associated with telomere length and implications for biobehavioral research. *Nurs. Res.* **63,** 36–50 (2014).

132. Liu, J. C. Y. *et al.* Absolute leukocyte telomere length in HIV-infected and uninfected individuals: evidence of accelerated cell senescence in HIV-associated chronic obstructive pulmonary disease. *PLoS One* **10,** e0124426 (2015).

133. Pathai, S. *et al.* Accelerated biological ageing in HIV-infected individuals in South Africa: a case-control study. *AIDS* **27,** 2375–84 (2013).

134. Xu, S. *et al.* Decreased telomere length in the small airway epithelium suggests accelerated aging in the lungs of persons living with human immunodeficiency virus (HIV). *Respir. Res.* **19,** 117 (2018).

135. Leung, J. M. *et al.* Longitudinal study of surrogate aging measures during human immunodeficiency virus seroconversion. *Aging (Albany. NY).* **9,** 687–705 (2017).

136. Gonzalez-Serna, A. *et al.* Rapid Decrease in Peripheral Blood Mononucleated Cell Telomere Length After HIV Seroconversion, but Not HCV Seroconversion. *JAIDS J. Acquir. Immune Defic. Syndr.* **76,** e29–e32 (2017).

137. O'Callaghan, N. J. & Fenech, M. A quantitative PCR method for measuring absolute telomere length. *Biol. Proced. Online* **13,** 3 (2011).

138. Kozich, J. J., Westcott, S. L., Baxter, N. T., Highlander, S. K. & Schloss, P. D. Development of a dual-index sequencing strategy and curation pipeline for analyzing amplicon sequence data on the MiSeq Illumina sequencing platform. *Appl. Environ. Microbiol.* **79,** 5112–20 (2013).

139. Zilberman-Schapira, G. *et al.* The gut microbiome in human immunodeficiency virus infection. *BMC Med.* **14,** (2016).

140. Twigg Iii, H. L., Weinstock, G. M. & Knox, K. S. Lung microbiome in human immunodeficiency virus infection. *Transl. Res.* 1–11 (2016). doi:10.1016/j.trsl.2016.07.008

Appendices

Appendix A Sample Metadata

Sample ID	Sample Type	HIV Status	Subject ID	Site	Age	Gender	DNA (ng/µL)
NNTC-fr01-DNA02	Lung	Positive	7102847472	Texas	54	Female	38.46
NNTC-fr02-DNA03	Small Intestine	Positive	7102847472	Texas	54	Female	167.29
NNTC-fr03-DNA02	Lung	Positive	1048	UCLA	43	Male	9.07
NNTC-fr04-DNA02	Lung	Positive	1071	UCLA	39	Male	110.50
NNTC-fr05-DNA02	Lung	Positive	1093	UCLA	56	Male	25.98
NNTC-fr06-DNA02	Lung	Positive	1115	UCLA	60	Male	7.36
NNTC-fr07-DNA02	Small intestine	Positive	1115	UCLA	60	Male	135.44
NNTC-fr08-DNA04	Lung	Positive	1133	UCLA	56	Male	67.61
NNTC-fr09-DNA05	Small intestine	Positive	1133	UCLA	56	Male	167.05
NNTC-fr10-DNA04	Lung	Positive	1134	UCLA	56	Female	105.13
NNTC-fr11-DNA02	Small intestine	Positive	1134	UCLA	56	Female	271.43
NNTC-fr12-DNA03	Lung	Negative	3002	UCLA	66	Male	69.07
NNTC-fr13-DNA04	Lung	Negative	3013	UCLA	64	Female	15.06
NNTC-fr14-DNA02	Lung	Negative	3015	UCLA	64	Female	45.13
NNTC-fr15-DNA02	Lung	Negative	3021	UCLA	69	Female	46.47
NNTC-fr16-DNA04	Lung	Negative	3029	UCLA	54	Male	63.44
NNTC-fr17-DNA02	Small intestine	Negative	3029	UCLA	54	Male	382.40
NNTC-fr18-DNA05	Lung	Negative	3030	UCLA	62	Female	337.32
NNTC-fr19-DNA06	Small intestine	Negative	3030	UCLA	62	Female	85.23
NNTC-fr20-DNA03	Lung	Negative	3031	UCLA	62	Female	17.93
NNTC-fr21-DNA04	Small intestine	Negative	3031	UCLA	62	Female	231.48
NNTC-fr22-DNA02	Lung	Negative	3032	UCLA	66	Male	57.07
NNTC-fr23-DNA02	Small intestine	Negative	3032	UCLA	66	Male	130.67
NNTC-fr24-DNA02	Lung	Negative	3033	UCLA	62	Female	92.25
NNTC-fr25-DNA03	Small intestine	Negative	3033	UCLA	62	Female	81.26
NNTC-fr26-DNA04	Lung	Negative	3035	UCLA	46	Male	25.37
NNTC-fr27-DNA02	Small intestine	Negative	3035	UCLA	46	Male	133.56
NNTC-fr28-DNA03	Lung	Negative	3038	UCLA	74	Female	59.59
NNTC-fr29-DNA04	Small intestine	Negative	3038	UCLA	74	Female	200.67
NNTC-fr30-DNA05	Lung	Negative	3041	UCLA	77	Female	159.78
NNTC-fr31-DNA03	Small intestine	Negative	3041	UCLA	77	Female	107.92
NNTC-fr32-DNA02	Lung	Positive	4015	UCLA	30	Male	34.09
NNTC-fr33-DNA04	Small intestine	Positive	4015	UCLA	30	Male	205.80
NNTC-fr34-DNA04	Lung	Positive	4028	UCLA	46	Female	31.92
NNTC-fr35-DNA02	Lung	Positive	4049	UCLA	44	Male	57.62
NNTC-fr36-DNA02	Lung	Positive	4067	UCLA	44	Male	111.23

NNTC-fr37-DNA02	Lung	Positive	4068	UCLA	41	Male	155.02
NNTC-fr38-DNA04	Lung	Positive	4084	UCLA	46	Male	81.62
NNTC-fr39-DNA03	Small intestine	Positive	4084	UCLA	46	Male	92.26
NNTC-fr40-DNA05	Lung	Positive	4090	UCLA	60	Male	1.34
NNTC-fr41-DNA02	Small intestine	Positive	4090	UCLA	60	Male	226.62
NNTC-fr42-DNA02	Lung	Positive	4115	UCLA	49	Male	0.10
NNTC-fr43-DNA03	Small intestine	Positive	4115	UCLA	49	Male	50.25
NNTC-fr44-DNA04	Lung (Left)	Negative	3010	UCLA	51	Female	112.60
NNTC-fr45-DNA02	Lung (Right)	Negative	3010	UCLA	51	Female	27.78
NNTC-fr46-DNA04	Lung (Left)	Negative	3039	UCLA	72	Female	70.66
NNTC-fr47-DNA05	Lung (Right)	Negative	3039	UCLA	72	Female	207.18
NNTC-fr48-DNA02	Small intestine	Negative	3039	UCLA	72	Female	106.93
NNTC-fr49-DNA02	Lung	Positive	MHBB714	Mount Sinai	37	Female	107.55
NNTC-fr50-DNA02	Small intestine	Positive	MHBB714	Mount Sinai	37	Female	125.45
NNTC-fr51-DNA04	Lung	Negative	MHBB715	Mount Sinai	85	Male	60.04
NNTC-fr52-DNA02	Small intestine	Negative	MHBB715	Mount Sinai	85	Male	105.49
NNTC-fr53-DNA04	Lung	Positive	10030	Mount Sinai	62	Male	8.20
NNTC-fr54-DNA02	Small intestine	Positive	10030	Mount Sinai	62	Male	63.62
NNTC-fr55-DNA01	Lung	Positive	1141	UCLA	44	Male	172.01
NNTC-fr56-DNA01	Small Intestine	Positive	1141	UCLA	44	Male	274.69
NNTC-fr57-DNA01	Lung	Positive	1142	UCLA	45	Male	95.41
NNTC-fr58-DNA01	Small Intestine	Positive	1142	UCLA	45	Male	452.63
NNTC-fr59-DNA01	Lung	Positive	1143	UCLA	64	Male	171.35
NNTC-fr60-DNA01	Small Intestine	Positive	1143	UCLA	64	Male	407.57
NNTC-fr61-DNA01	Lung	Positive	1166	UCLA	52	Male	236.25
NNTC-fr62-DNA01	Small Intestine	Positive	1166	UCLA	52	Male	263.53
NNTC-fr63-DNA01	Lung	Positive	1174	UCLA	41	Male	172.28
NNTC-fr64-DNA01	Small Intestine	Positive	1174	UCLA	41	Male	569.87
NNTC-fr65-DNA01	Lung	Positive	1182	UCLA	54	Male	92.62
NNTC-fr66-DNA01	Small Intestine	Positive	1182	UCLA	54	Male	310.88
NNTC-fr67-DNA01	Lung	Positive	2092	UCLA	41	Male	224.11
NNTC-fr68-DNA01	Small Intestine	Positive	2092	UCLA	41	Male	313.71
NNTC-fr69-DNA01	Lung	Negative	3009	UCLA	53	Female	378.75
NNTC-fr70-DNA01	GI	Negative	3009	UCLA	53	Female	89.81
NNTC-fr71-DNA03	Lung	Positive	4127	UCLA	46	Male	10.98
NNTC-fr72-DNA01	Small Intestine	Positive	4127	UCLA	46	Male	78.58
NNTC-fr73-DNA01	Lung	Positive	4129	UCLA	59	Female	191.57
NNTC-fr74-DNA01	Small Intestine	Positive	4129	UCLA	59	Female	133.04
NNTC-fr75-DNA01	Lung	Positive	5058	UCLA	68	Male	130.16
NNTC-fr76-DNA01	Small Intestine	Positive	5058	UCLA	68	Male	295.97

NNTC-fr77-DNA01	Lung	Positive	10266	Mount Sinai	59	Female	121.60
NNTC-fr78-DNA01	Small Intestine	Positive	10266	Mount Sinai	59	Female	102.89
NNTC-fr79-DNA01	Lung	Negative	40020	Mount Sinai	21	Female	221.28
NNTC-fr80-DNA01	Small Intestine	Negative	40020	Mount Sinai	21	Female	59.90
NNTC-fr81-DNA01	Lung	Negative	mhbb723	Mount Sinai	58	Female	143.94
NNTC-fr82-DNA01	Small Intestine	Negative	mhbb723	Mount Sinai	58	Female	41.70
NNTC-fr83-DNA01	Lung	Negative	mhbb724	Mount Sinai	62	Male	208.69
NNTC-fr84-DNA01	Small Intestine	Negative	mhbb724	Mount Sinai	62	Male	59.63
NNTC-fr85-DNA01	Lung	Positive	7201068268	Texas	42	Male	150.30
NNTC-fr86-DNA01	Small Intestine	Positive	7201068268	Texas	42	Male	300.35